Geol. Mag. **149** (*4*), *2012, pp. 696–721. © Cambridge University Press 2011*
doi:10.1017/S0016756811000835

New palaeomagnetic, petrographic and $^{40}Ar/^{39}Ar$ data to test palaeogeographic reconstructions of Caledonide Svalbard

KRZYSZTOF MICHALSKI*†, MAREK LEWANDOWSKI‡ & GEOFF MANBY§

*Institute of Geophysics, Polish Academy of Sciences, ul. Ksiecia Janusza 64, 01-452 Warsaw, Poland
‡Institute of Geological Sciences, Polish Academy of Sciences, ul. Twarda 51/55, 00-818 Warsaw, Poland
§Natural History Museum, Mineralogy Department, Cromwell Road, London, SW7 5BD, UK

(*Received* 6 January 2011; *accepted* 19 July 2011; *first published online* 14 November 2011)

Abstract – New palaeomagnetic and petrographic data are presented from Cambrian rocks of SW Svalbard to test, for the first time, Palaeozoic reconstructions of the major terranes of Svalbard. In the course of thermal demagnetization three ChRM (characteristic remanent magnetization) components were identified, which were labelled HORNL, HORNM and HORNH, respectively, on the basis of their different unblocking temperatures. The HORNM magnetization is related to the Late Ordovician–Silurian formation of the synmetamorphic S_1 foliation. The HORNM palaeopole ($\Phi = -18.5^\circ$, $\Lambda = 359^\circ$, $D_p/D_m = 5.8^\circ/11.4^\circ$, Plat = 6° N) matches exactly the Silurian sectors of the Baltica–Laurentia apparent polar wander paths after the closure of Iapetus (455–415 Ma). The 450 Ma ^{40}Ar–^{39}Ar age determination from mica ages obtained from the broad zone of mylonites along the Billefjorden Fault Zone which separates the Central and Eastern terranes, also suggests that the two terranes were eventually amalgamated by 450 Ma. The $HORNM_{VGP}$ also lies very near the palaeopole derived from the Middle Proterozoic rocks of the Eastern Terrane (Ny Friesland), metamorphosed during Caledonian time, suggesting its close proximity to the study area (Central Terrane). The present study has shown that at least two of the major terranes of Svalbard, as defined by previous authors, occupied similar geographical locations by Silurian time, and the previously proposed large-scale Late Devonian left lateral displacements are not supported.

Keywords: Arctic Caledonides, palaeomagnetism, Laurentia–Baltica–Svalbard relations, Late Ordovician–Late Silurian amalgamation.

1. Introduction

The Svalbard Archipelago, which lies on the north-western corner of the Barents Sea–East European Platform (Fig. 1), has a pre-Caledonian basement that consists of a mosaic of crustal blocks or 'terranes' that differ significantly in their lithological, tectonic and metamorphic characteristics (e.g. Harland, 1997; Gee & Tebenkov, 2004). These crustal blocks are separated by major, N–S-trending fault zones that are commonly taken to represent the terrane boundaries (Harland & Wright, 1979; Harland, 1997; Mazur *et al*. 2009). Although much has been done to correlate the lithologies and tectonothermal events exhibited by the Svalbard terranes with those found in similar aged rocks in the Laurentian and Baltican plates, the Early Palaeozoic positions of the Svalbard terranes and the timing of their final amalgamation remains controversial (e.g. Birkenmajer, 1975; Harland & Wright, 1979; Harland, 1997; Lyberis & Manby, 1999; Gee & Tebenkov, 2004).

According to Harland & Wright (1979) and Harland (1997) the major terranes of Svalbard occupied widely disparate positions along the eastern and northeastern margins of Greenland until Late Devonian times (Fig. 2a). The amalgamation of these terranes was accommodated by large-scale (*c*. 1000 km) sinistral strike slip motion along the bounding fault zones after the main collision between Baltica and Laurentia. Gee & Page (1994), Lyberis & Manby (1999) and Gee & Tebenkov (2004) have suggested, alternatively, that most of the Svalbard terranes were already amalgamated by Late Silurian time off the NE Greenland margin. The tectonic escape-like motions along the bounding faults and final assembly of the Svalbard terranes are interpreted to be a consequence of the oblique Baltica–Laurentia collision (Gee & Page, 1994; Lyberis & Manby, 1999).

While most reconstructions consider the Svalbard terranes to have been distributed along the eastern margin of Laurentia until Late Palaeozoic time, the timing of their incorporation into Baltica remains unresolved (Roberts, 2003; Torsvik & Cocks, 2005; Cocks & Torsvik, 2005). The location of the Baltica–Laurentia suture also remains controversial, with some authors suggesting that it cuts the Svalbard block at depth beneath the Billefjorden Fault Zone (BFZ; Breivik *et al*. 2002, 2003) or that it was situated on the Barents Shelf between Scandinavia, Svalbard and Franz Joseph Land (e.g. Harland & Gayer, 1972; Gee & Tebenkov, 2004). The presence of meta-igneous complexes with destructive plate margin affinities

†Author for correspondence: krzysztof.michalski@igf.edu.pl

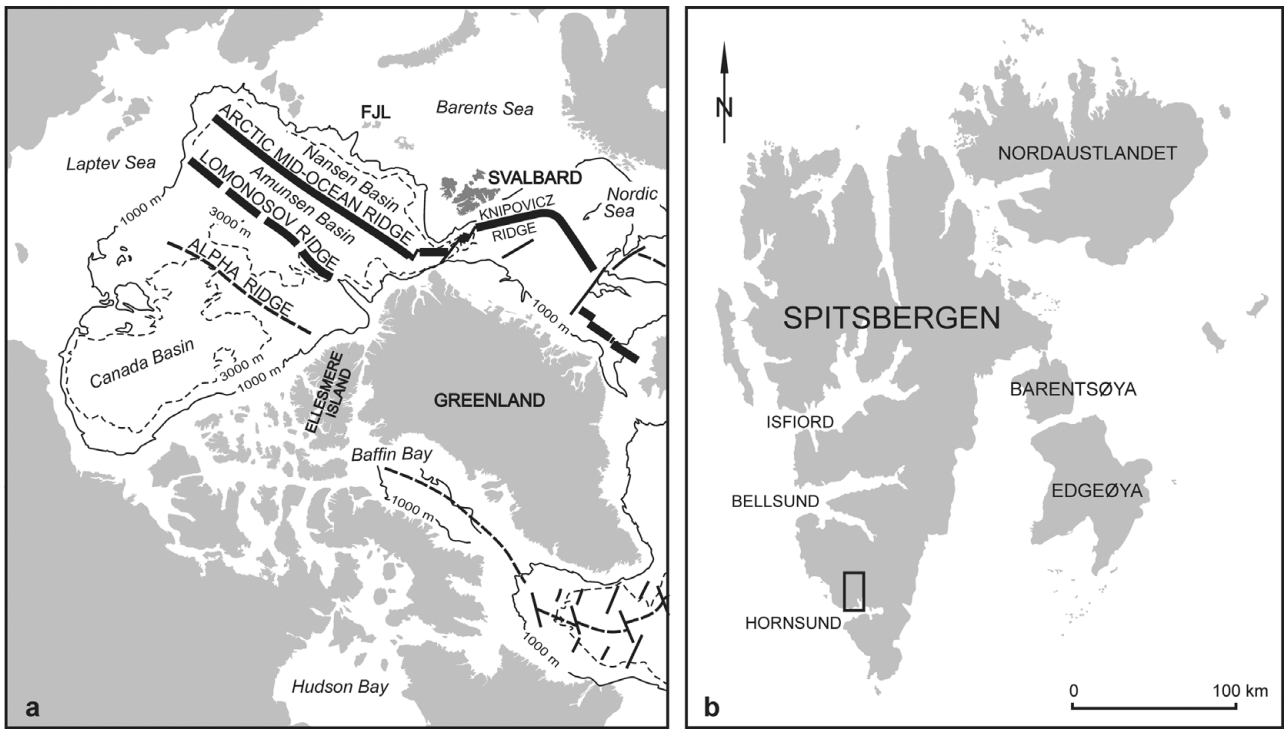

Figure 1. (a) Location of Svalbard in the present Northern Atlantic/Arctic geotectonic system (map after Srivastava, 1985); FJL – Franz Joseph Land. (b) Contour map of the Svalbard Archipelago; the area of investigation is marked by a square.

such as the Vestgötabreen blueschists (Horsfield, 1972; Manby, 1978; Ohta, 1979; Hirajima *et al*. 1988) of Central Western Svalbard, while clearly representing a subduction zone fragment, do little to inform us as to the position of the suture because of subsequent tectonism. Offshore seismic reflection profiling (Breivik *et al*. 2005; Barrére, Ebbing & Gernigon, 2009) on the Barents Shelf to the south of Svalbard and the aeromagnetic studies (Skilbrei, 1992) have also failed to confirm, unequivocally, the geographic position of the suture. What is certain is that Svalbard is traversed by major N–S-trending fault zones that are associated with abundant evidence of ductile to brittle sinistral shearing, and retrogression of higher grade metamorphic mineral assemblages imposed, without exception, in Caledonian time (*sensu lato*; see Manby, 1990; Lyberis & Manby, 1999).

Since palaeomagnetism is the only method capable of quantifying the past coordinates of crustal blocks, it would appear, therefore, to present an ideal means to test the various hypotheses concerning the Late Precambrian–Palaeozoic palaeogeography of Svalbard. There is, however, an important limitation to this method in that the Caledonian metamorphism and deformation has extensively altered the relevant rocks' materials throughout Svalbard. As the palaeomagnetic record is based on the rule of 'closure process', taking place at the critical temperature below which the system of magnetic domains became stable (e.g. Butler, 1992, pp. 56–64; Tauxe, 1996, pp. 57–8; Dunlop & Özdemir, 1997, pp. 201–62), the characteristic remanent magnetization (ChRM) components which were magnetized before Caledonian heating and deformation events could be overprinted by younger directions. Although there may be some Lower Palaeozoic sequences still carrying the primary ChRM components, it is likely that the primary pre-Caledonian directions have been re-magnetized completely. Nonetheless, even in these places secondary components, related to Caledonian thermal events, can still provide some important constraints on the reconstructions, when they are supported by robust isotopic age determinations.

In this contribution new palaeomagnetic data are presented from Cambrian rocks of the Hornsund region of SW Svalbard (Fig. 1b) that focus, for the first time, on the Lower Palaeozoic palaeomagnetic record of Svalbard in the context of the major Caledonian metamorphic and tectonic events. Investigations of the natural remanent magnetization (NRM) vectors have been supported by detailed rock magnetic, optical microscope, scanning electron microscope (SEM) and electron-probe microanalyses.

The results of ^{40}Ar–^{39}Ar isotope analyses from mylonites developed along the BFZ are discussed here together with additional field and published palaeomagnetic data from Ny Friesland (Eastern Terrane), which lies between Baltica and the Hornsund region (Central Terrane), as they will shed further light on the timing of movement along the BFZ and the amalgamation of the Central and Eastern Terranes of Svalbard.

This study is part of an on-going project that seeks to reconstruct the changing positions of the major terranes of Svalbard in the Late Precambrian–Late Palaeozoic interval.

https://doi.org/10.1017/S0016756811000835 Published online by Cambridge University Press

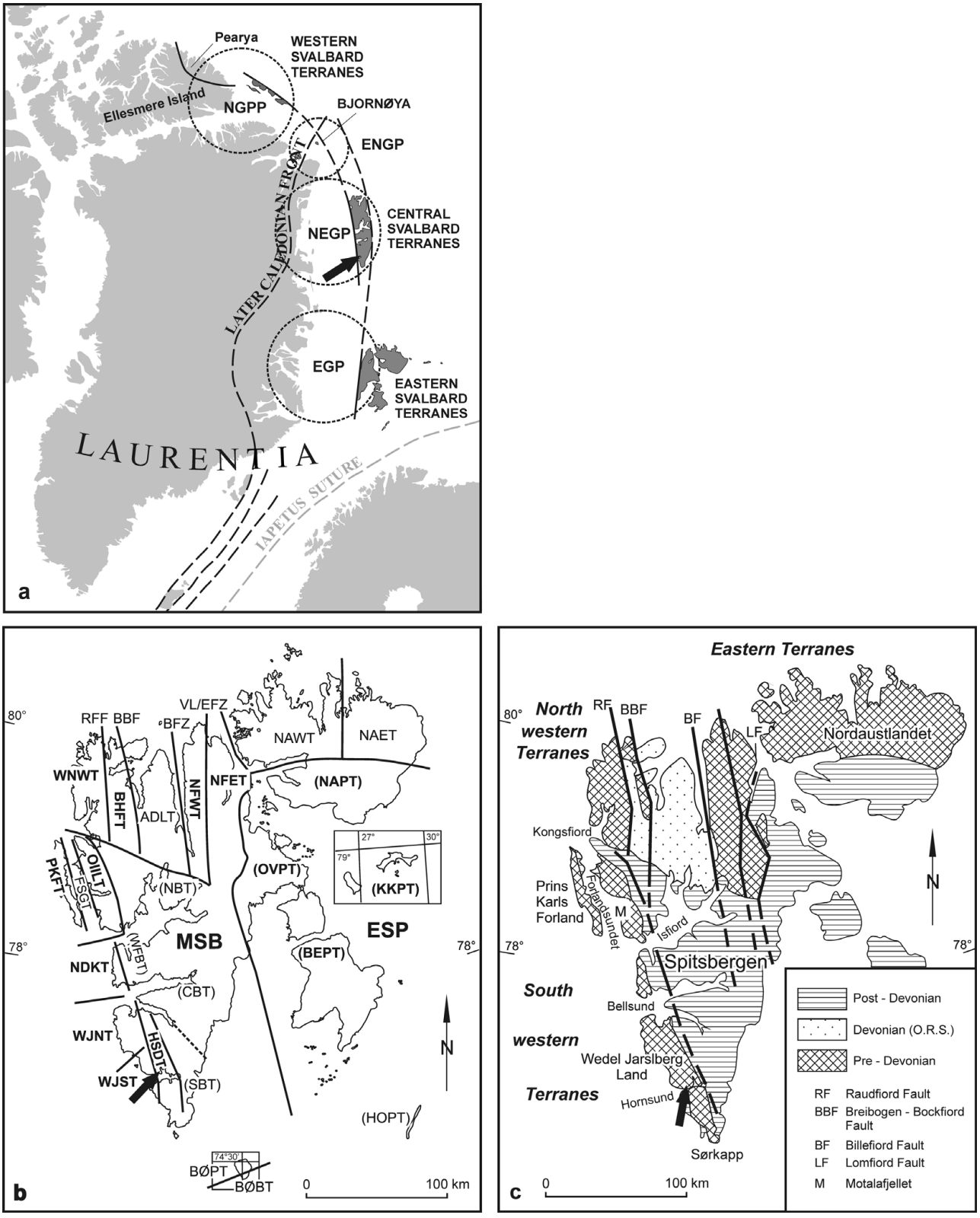

Figure 2. (a) Dispersion of Svalbard terranes along the margins of Greenland in Silurian times (after Harland, 1997); provinces are encircled: EGP – East Greenland Province; NEGP – Northeast Greenland Province; ENGP – Eastern North Greenland Province; NGPP – North Greenland–Pearya Province. (b) Terranes of Svalbard; division after Harland (1997); abbreviations: **Eastern basement terranes**: NAET – Nordaustlandet Eastern Terrane; NAWT – Nordaustlandet Western Terrane; NFET – Ny Friesland (including Olav V Land) Eastern Terrane; NFWT – Ny Friesland Western Terrane. **Central basement terranes:** ADLT – Andrèe Land-Dickson Land Terrane; BHFT – Biskayerfonna–Holtedahlfonna Terrane; WNWT – Northwest Spitsbergen Terrane; HSDT – Hornsund Terrane. **Western basement terranes:** PKFT – Prins Karls Forland Terrane; FSGT – Forlandsundet Graben Terrane; OIILT – Oscar II Land Terrane; NDKT – Nordenskiöldkysten–Nordenskiöld Land Terrane; WJNT – NW Wedel Jarlsberg–North of Torellbreen Terrane; WJST – SW Wedel Jarlsberg Land–South of Torellbreen Terrane. **Southern basement terrane:** BØBT – Bjørnøya Basement Terrane**. Cover terranes:** (post-Devonian sequences): CBT – Central Basin Terrane; NBT – North Basin Terrane; WFBT – Western Fold

https://doi.org/10.1017/S0016756811000835 Published online by Cambridge University Press

2. Tectonic setting and structure

The main target area for the present study is located in the southeastern part of Wedel Jarlsberg Land, north of Hornsund, Southern Spitsbergen (Fig. 1b). Tectonostratigraphically, the Lower Palaeozoic rocks of this region belong to the Hornsund Terrane (HSDT; see Harland, 1997), which constitutes part of the Central Terrane of Svalbard (CTS; Harland & Wright, 1979; Fig. 2b). Following Harland (1997), the western boundary of the HSDT is defined by the NNW–SSE-trending Kongsfjord–Hansbreen Fault Zone (KHFZ). West of this fault is the Wedel Jarlsberg Land–South of Torellbreen Terrane (WJST), which forms part of the Western Terrane of Svalbard (WTS; Harland & Wright, 1979). Gee & Tebenkov (2004) do not consider, however, the KHFZ to be an important structure, but regard the pre-Devonian sequences of Central and SW Spitsbergen to constitute the Southwestern Terrane (Fig. 2c). Although the eastern boundary of the Palaeozoic HSDT (or Central Terrane) is buried beneath the Upper Palaeozoic–Mesozoic rocks in SW Spitsbergen, it is exposed to the north as the BFZ; this is described further in a later section.

Lithostratigraphically, the Lower Palaeozoic succession of Hornsund has been divided into the Cambrian (Sofiekammen Group) and the Ordovician (Sörkapp Land Group), which are separated by the Hornsundian unconformity (Birkenmajer, 1978). The youngest Lower Palaeozoic rocks in the area are the Lower Ordovician Hornsundtinden limestones. Upper Ordovician and Silurian sequences are not preserved, and were probably eroded after the Caledonian uplift (Birkenmajer, 1990; Ohta & Dallman, 1994). Trilobite fauna, showing Laurentian affinity and belonging to the *Bonnia–Olenellus* Zone (Birkenmajer & Orłowski, 1977), have been found in scree from the exposures of the Slaklidalen Formation, suggesting late Early Cambrian deposition (Harland, 1997).

The limestones of the Slaklidalen Formation (Sofiekammen Group), which were sampled for palaeomagnetic analysis (Fig. 3), are exposed on the opposite limbs of the Sofiekammen syncline (Birkenmajer, 1978). The Sofiekammen syncline (Figs 3, 4a, b), in common with all of the major Caledonian fold structures of the Sofiekammen Group in Wedel Jarlsberg Land, is overturned with an eastward vergence.

Structurally, the Sofiekammen syncline, an F_1 Caledonian fold, appears to have formed initially by a flexural slip mechanism modified by flattening and shearing as the fold 'locked-up' (Fig. 4b). In thin-section, the limestones exhibit a pervasive syntectonic, metamorphically driven, recrystallization of the matrix carbonate and ferromagnetic phases to produce a strong dimensional preferred orientation that defines the S_1 axial planar foliation to this fold (Fig. 5). The sampled KAMB KAL A (Fig. 5) carbonate segregations, which lie in the S_1 foliation, are rotated, flattened and sheared tension gashes that formed at an early (flexural slip) stage in the formation of the fold. The S_1 cleavage is also affected by some weak kink-like centimetre-scale folding (Fig. 5d).

The later KAMB KAL B sampled veins (Fig. 5), which cut the S_1 axial planar cleavage surfaces, including the crenulation folds, are seen to be traversed occasionally by shear and pressure solution (stylolitic) surfaces, suggesting that these features formed at some late stage in the development of the S_1 foliation. These veins are particularly concentrated on the shallow eastern limb of the Sofiekammen syncline. The rocks dip shallowly to the west, and the vein arrays reflect extension (Fig. 5c), possibly induced by nappe stacking and flattening of this fold limb. The high angle, with respect to the shallow S_1, extensional fractures generated by the flattening became sites of the KAMB KAL B type carbonate-ferromagnetic mineral precipitation (Fig. 5a, e).

The limestones have recrystallized and they often exhibit sedimentary and tectonically induced brecciation that pre-dates the final development of the S_1 foliation. Microscopic and microprobe observations reveal that these tectonized zones are enriched in silica, clay minerals, organic matter, dolomites, Fe sulphides and Fe, Ti oxides (Fig. 6c).

Subsequent post-Caledonian deformation events have affected much of the western and northern part of Svalbard including the rocks of the target area. The first deformation event is referred to as the Svalbardian folding or diastrophism and it is well recorded in the Devonian basin fill of Northern Svalbard (e.g. Manby & Lyberis, 1992; Harland, 1997). Devonian (Emsian) rocks, affected by deformation attributed to the Svalbardian event, are also found in SW Spitsbergen (Birkenmajer, 1964), where they occupy a much smaller area than those to the north.

The Late Cretaceous–Early Paleocene West Spitsbergen Fold Belt (WSFB) deformation event was much more intense than that of Svalbardian age. It produced typical foreland fold-and-thrust belt structures, developed in the Upper Palaeozoic to Mesozoic rocks to the east of the study area. The effect of the WSFB deformation on the target rocks in the study area appears to have been confined largely to rigid block

Belt/Basin Terrane; SBT – Southern Basin Terrane; NAPT – Nordaustlandet Platform Terrane; OVPT – Olav V Land Platform Terrane; BEPT – Barentsøya and Edgeøya Platform Terrane; KKPT – Kong Karls Land Platform Terrane; HOPT – Hopen Platform Terrane; BØPT – Bjørnøya Platform Terrane; MSB – Main Spitsbergen Basin; ESP – Eastern Svalbard Platform. **Fault Zones:** RFF – Raudfjorden; BBF – Breibogen; BFZ – Billefjorden; VL/EFZ – Veteranen Line (name after Harland, 1997)/Eolussletta Fault Zone (name after Lyberis & Manby, 1999). (c) Terranes of Svalbard; division after Gee & Teben'kov (2004); in all three presented maps the sampled area is indicated by arrows.

https://doi.org/10.1017/S0016756811000835 Published online by Cambridge University Press

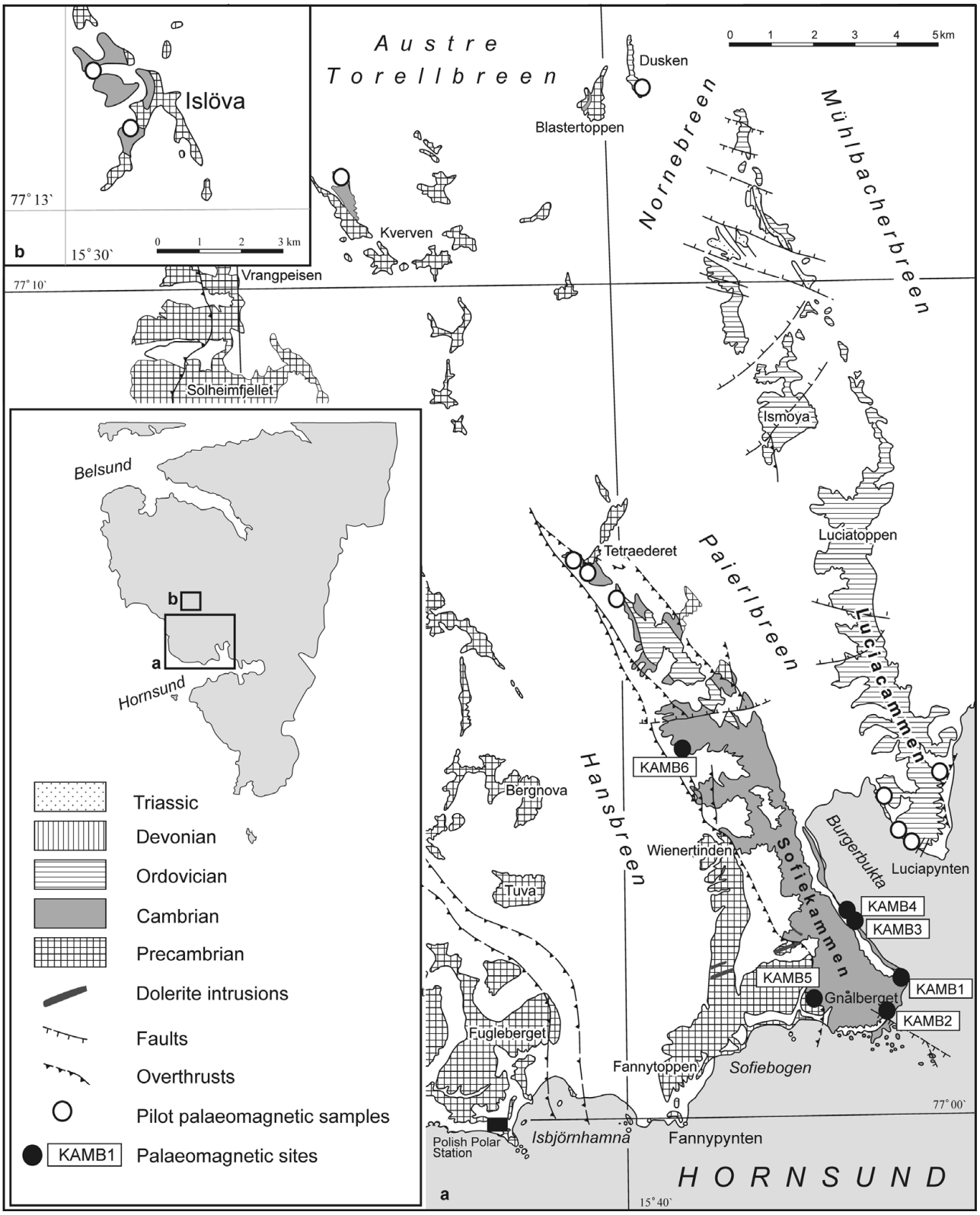

Figure 3. Geological map of southwestern Wedel Jarlsberg Land (after Birkenmajer, 1978); open circles indicate the locations where the pilot palaeomagnetic samples were collected in 1999–2000; palaeomagnetic sites collected in 2002 and 2004, situated on the opposite limbs of the Sofiekammen syncline, are marked by dots.

movements accommodated, at least in part, by the reactivation of pre-existing faults.

No thermally induced recrystallization or neomineralization (i.e. metamorphism) has been reported in the literature from any of the Upper Palaeozoic–Mesozoic rocks affected by the Svalbardian or the WSFB deformation events. Tessensohn, Henes-Kunst & Krumm (2001), using K/Ar techniques, concluded

https://doi.org/10.1017/S0016756811000835 Published online by Cambridge University Press

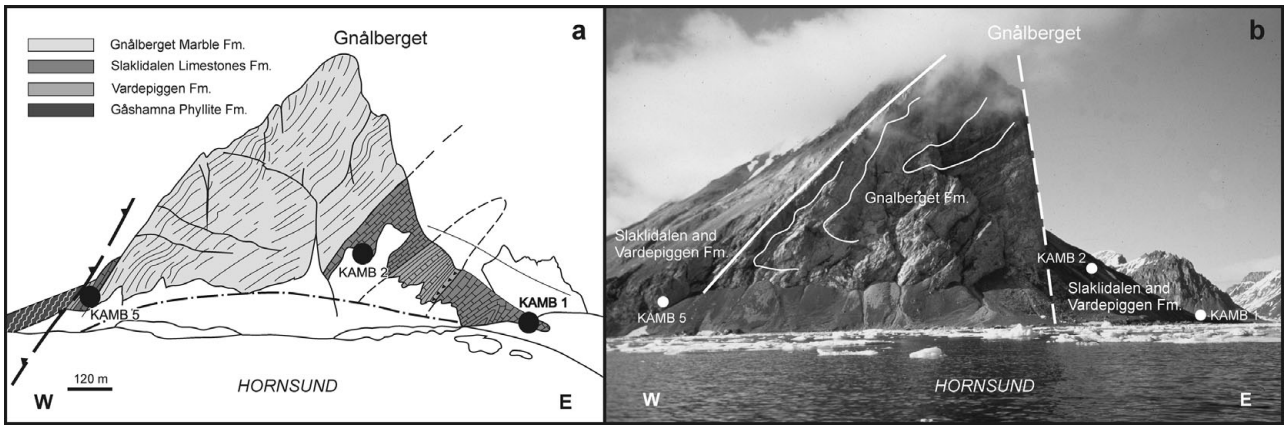

Figure 4. (a) Cross-section through the Sofiekammen syncline (after Birkenmajer, 1978). (b) Photograph of the Sofiekammen syncline exposed on south slopes of Gnålberget, Hornsund; note that the syncline is overturned indicating tectonic transport to the east; on both cross-section and photograph palaeomagnetic sites KAMB 1, 2 and 5 are marked by dots.

that the rocks of the WSFB, including SW Spitsbergen, and the Central Tertiary Basin never reached temperatures sufficient to cause any detectable recrystallization/neomineralization during their deformation.

A number of thermal events have occurred, however, within the Svalbard Archipelago at various intervals since Caledonian time. These events include Late Caledonian–Devonian granite plutons intruded into the Proterozoic rocks of NW Spitsbergen, Ny Friesland and Nordaustlandet, intrusion of Late Jurassic–Early Cretaceous basaltic dykes and sills at Hinlopenstretet (Halvorsen, 1989), Central (Vincenz *et al*. 1984) and Southern Spitsbergen (Vincenz *et al*. 1981) and eruption of Neogene lavas exposed in Andree Land (Harland, 1997). Of these events, only the Late Caledonian (*sensu lato*) granite intrusions and associated migmatites of NW Spitsbergen (Harland, 1997 and references therein) were associated with any extensive tectonothermal activity, albeit restricted to that terrane. The other igneous events are associated with only limited or no recognizable recystallization in the host rocks.

3. Sampling and laboratory procedures

3.a. Sampling and preparation for palaeomagnetic analyses

Field investigations in the area of Hornsund were undertaken in three stages. During the 1999–2000 season, 30 non-oriented pilot samples from five Lower Palaeozoic carbonate formations (Blåstertoppen Fm, Nordstetinden Fm, Slaklidalen Fm, Luciapynten Fm and Dusken Fm) were collected. The locations of the sampling sites in the Hornsund Terrane are shown in Figure 3. To select the most useful rocks for palaeomagnetic procedures, the following elements were investigated: (1) the intensity and structure of NRM; (2) changes of the magnetic susceptibility in the course of the thermal demagnetization process; and (3) the magnitude of the P′ parameter (corrected anisotropy degree after Jelinek, 1977).

The limestones of the Slaklidalen Fm appeared to be the most promising for further analyses for the following reasons:

(i) The NRM components could be defined with high precision (in 90 % of samples angular standard deviation (ASD) $< 5^{\circ}$), up to the final stages of the demagnetization process, when the intensity of NRM decreased below $5^{*}10^{-3}$ μA/m.

(ii) There was no significant change in the bulk susceptibility during thermal demagnetization suggesting that during heating the ferromagnetic mineral assemblages remained unchanged.

(iii) Of the samples investigated, 70 % revealed a susceptibility signal below $10^{*}10^{-6}$ SI that resulted in large errors of anisotropy parameters. In the remaining 30 % of the samples with the susceptibility signal around $50–100^{*}10^{-6}$ SI the P′ parameter was below 1.05, suggesting that the stress factor had only a minor, if any, influence on the alignment of the ferromagnetic fabric (Tarling & Hrouda, 1993).

Fieldwork in 2002 and 2004 concentrated on sampling the Slaklidalen Fm from the Caledonian Sofiekammen syncline (Figs 3, 4) with two sites on the steep overturned western limb and four sites on the shallow un-inverted eastern limb (Fig. 4). Each of the sites was 5–10 m in diameter and included three to five beds. A total of 41 palaeomagnetic rock samples with the minimum dimension of 15 cm^2 were independently oriented using a magnetic compass and retrieved from the fresh rock using a geological hammer (6–7 block samples from each site).

Cylindrical samples for further analyses were prepared in the Department of Geomagnetism Laboratory of Palaeomagnetism, at the Institute of Geophysics, Polish Academy of Science (IGF PAS). From each of 41 oriented blocks up to five cylindrical cores 2.4 cm in diameter and 2.2 cm in length were drilled for the Lowrie test (*sensu* Lowrie, 1990) and demagnetization experiments. From each site additional small cylindrical cores (6 × 8 mm) and irregular samples up to 1 mm in diameter were prepared for rock magnetic study.

https://doi.org/10.1017/S0016756811000835 Published online by Cambridge University Press

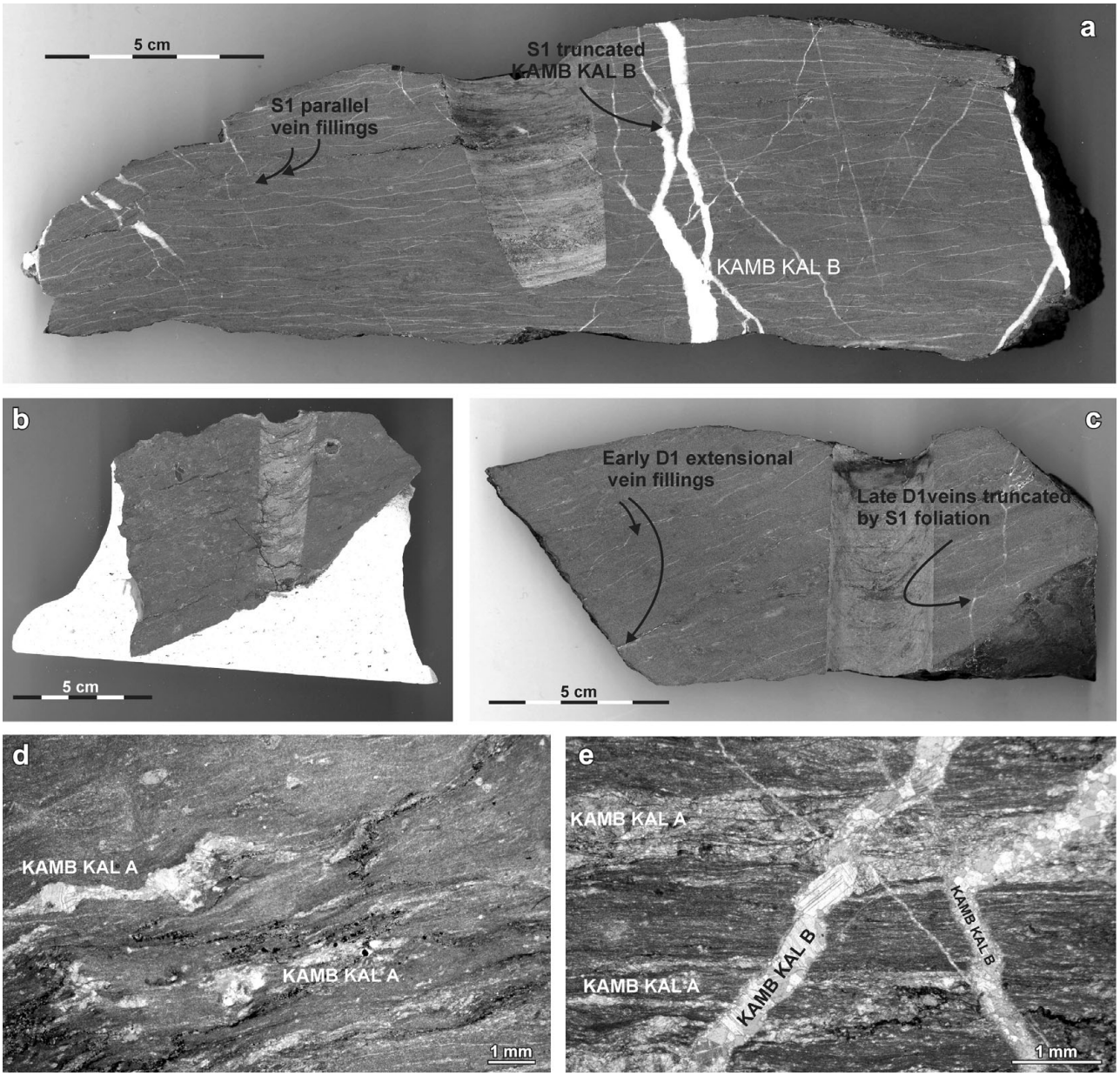

Figure 5. Textures of Slaklidalen Formation samples. (a) Early S_1 parallel veins which may indicate high pore fluid pressures during their formation. KAMB KAL B veins that cut S_1 at a high angle are themselves truncated by S_1 suggesting a late D_1 origin (macro section). (b) Limestone with synsedimentary breccia fabric. The S_1 foliation and numerous early vein fillings wrap around the breccia fragments (macro section). (c) Early D_1–F_1 extensional veins rotated and flattened. The later veins cut the S_1 foliation at a high angle but are themselves truncated by S_1 in places indicating that deformation continued after these veins formed (macro section). (d) KAMB KAL A is seen as recrystallized, boudinaged, slightly folded and sheared relics of sigmoidal tension gashes that most likely originated early in the formation of the F_1 Sofiekammen syncline. Also visible are traces of minor intrafolial F_1 folds defined by concentrations of opaque iron ore minerals. The entire F_1 axial planar foliation (S_1) is mylonitic in character and the KAMB KAL A infillings have been rotated in near parallelism with the S_1 foliation, which also exhibits some weak crenulation-like (F_2) folds. These folds may simply be the result of the shearing process rather than a separate and later fold phase. All of this deformation would have coincided with the main Caledonian (M_1) metamorphic event as the fold was progressively deformed (thin-section, Olympus binocular, transparent light). (e) KAMB KAL A is S_1 parallel as in (d) while KAMB KAL B clearly cuts the S_1 foliation. The KAMB KAL B veins, however, have been recrystallized and they are displaced by the S_1. The KAMB KAL B veins are also cut by stylolitic surfaces indicating that they are late D_1–F_1–S_1 and were emplaced before the S_1 fabric was fully developed. The thinner high-angle veins that truncate the S_1, which are themselves cut by KAMB KAL B veins, show small-scale crenulations that were certainly formed as a result of S_1 parallel shearing combined with pressure solution generated volume loss. All of these structures reflect the continuing and progressive deformation of the Sofekammen syncline, which formed during the synkinematic Caledonian metamorphism (thin-section, Olympus binocular, transparent light).

3.b. Identification of magnetic minerals

An initial evaluation of maximum unblocking temperatures ($T_{ub\ max}$) of ferromagnetic minerals was based on SIRM (saturation isothermal remanent magnetization) decay curves (procedure after Kądziałko-Hofmokl & Kruczyk, 1976). Small cylindrical cores (6 × 8 mm)

https://doi.org/10.1017/S0016756811000835 Published online by Cambridge University Press

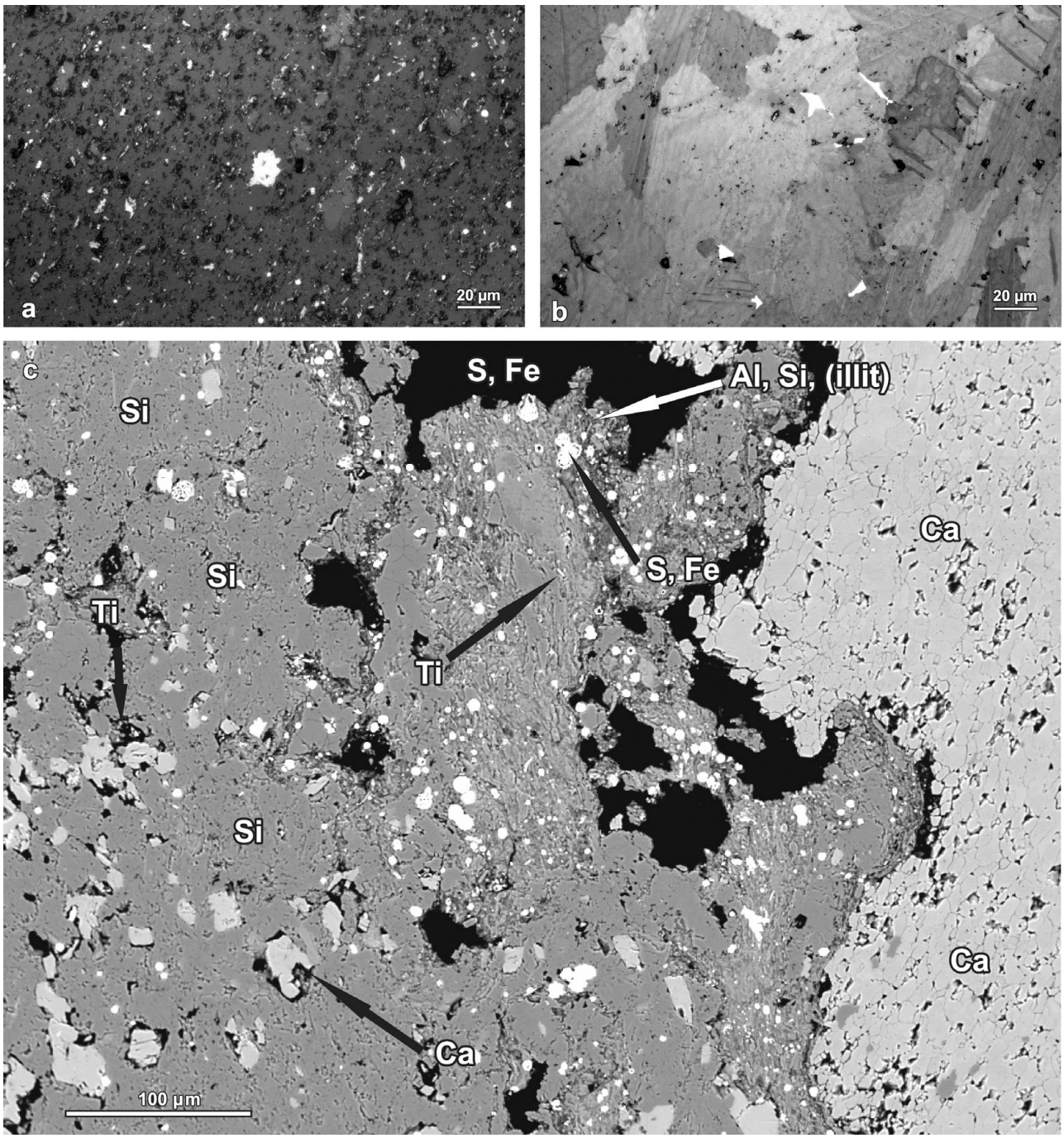

Figure 6. Ferromagnetic minerals distribution in Slaklidalen Fm samples. (a) Grains of magnetite (GEN A) in recrystallized carbonate matrix (thin-section, NIKON ore microscope, reflected light). (b) Grains of magnetite (GEN C) within calcite veins KAMB KAL B. The calcite has clearly recrystallized. The ferromagnetic grains have remained *in situ* and appear to have been enclosed by the recrystallized calcite with little or no re-orientation (thin-section, NIKON ore microscope, reflected light). (c) Fe, Ti oxides and Fe sulphides (GEN B) in the tectonized and brecciated fragments of sampled limestones (thin-section, BSE microprobe image; chemical composition of selected grains has been estimated by EDS analyses).

were magnetized in a 7 T field using a MMPM–10 (magnetic measurements pulse magnetizer). The cores were subsequently heated in the furnace combined with a spinner magnetometer up to 700 °C in a field-free space. The decay of the initial magnetic signal during heating and identification of the $T_{ub\,max}$ of particular magnetic minerals found in the samples could be observed on the thermal demagnetization curves (Fig. 7).

A more detailed determination of $T_{ub\,max}$ and coercivity spectra of ferromagnetic minerals was based on the three-component IRM (isothermal remanent magnetization) procedure described by Lowrie (1990). At first, 21 cylindrical cores (2.4 × 2.2 cm) representing all six sites were subjected to gradual magnetization along the *z*-axis at room temperature up to 2.9 T (limit of the coercivity of hard magnetic phases like haematite) using the MMPM–10 magnetometer. After

https://doi.org/10.1017/S0016756811000835 Published online by Cambridge University Press

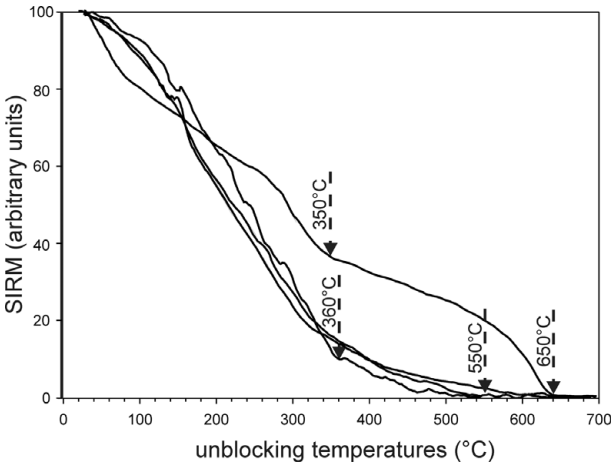

Figure 7. Examples of SIRM (saturation isothermal magnetization) analyses of the Slaklidalen Fm samples. Characteristic temperatures on demagnetization curves reflecting unblocking temperatures of ferromagnetic minerals existing in the samples are indicated by arrows.

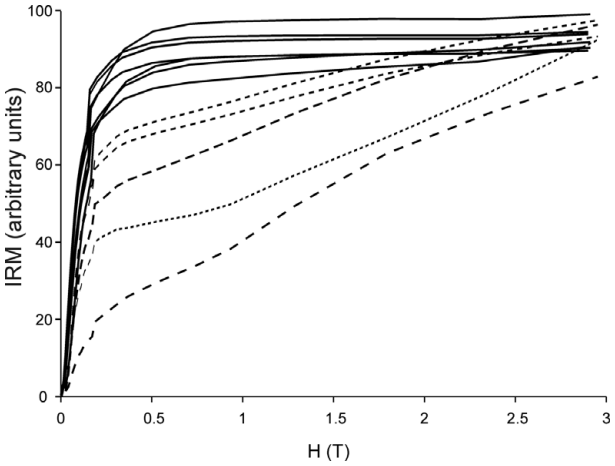

Figure 8. Examples of IRM (isothermal remanent magnetization) analysis of Slaklidalen Fm samples. Dotted lines represent samples that were not saturated in the maximum applied field (H = 2.9 T).

each magnetization step the IRM of the samples was measured on the Superconducting Quantum Interference Device (SQUID, 2G Enterprise model 755, USA) with a residual internal field of below 3 nT and a noise level of about 5 μA/m. The induced IRM versus increasing applied field diagrams (Fig. 8) provided the first estimation of coercivities of the samples.

The cores were then magnetized along two mutual perpendicular axes in fields of 0.4 T along the *y*-axis and 0.12 T (limit of the coercivity of soft magnetic phases like magnetite) along the *x*-axis. In the final stage of the experiment samples were subjected to a stepwise thermal demagnetization in a field-free magnetic furnace MMTD1 (Magnetic Measurements Thermal Demagnetizer of Great Britain). After each demagnetization step the magnetic signal of each of the samples was measured on the SQUID. The thermal demagnetization of the three orthogonal components of the composite SIRM provided an estimate of the relative quantities and unblocking temperature spectra of the magnetic phases present (Fig. 9).

Magnetic analyses were supported by observations of the rock microstructures, and the ferromagnetic minerals were identified using an optical microscope, SEM and electron microprobe techniques in the Department of Geology, University of Warsaw and in the Institute of Geological Sciences at the Polish Academy of Sciences. EDS (energy dispersive spectroscopy) and WDS (wavelength dispersive spectroscopy) microprobe analyses were also conducted on polished sections and the magnetic residuum of sampled rocks. To prepare the residuum, the limestones were dissolved in 10 % ethanoic acid (acetic acid). The Fe particles were then separated using a neodymium magnet.

3.c. Palaeomagnetic procedures

A total of 101 cylindrical cores (diameter: 2.2 cm; height: 2.6 cm) representing all six palaeomagnetic sites (16–17 cores from each site) were subjected to stepwise demagnetization. At first 18 cores representing four sites were subjected to stepwise alternating field (AF) demagnetization in the fields from 0 up to 40 mT. Then all cores were demagnetized thermally in the MMTD1 furnace. The specimens were heated in steps of 20–50 °C up to 500 °C, and after each step cooled to the room temperature in a zero magnetic field. After each demagnetization step the residual magnetic remanence was measured using the SQUID.

The thermal demagnetization process, together with the magnetic susceptibility (κ) of the cores, was monitored using a Czech low-field KLY-2 susceptibility bridge, since changes of the κ parameter reflect changes in magnetic mineral assemblages of the samples during heating.

To plot the demagnetization data and for calculating the ChRM components for particular samples, Palaeomagnetic Data Analysis software by Lewandowski, Werner & Nowożyński (1997), employing principal component analysis (PCA) after Kirschvink, (1980), was used. The ChRM components were determined on Zijderveld diagrams as a direction of best fit line to a minimum of three points, with an ASD not exceeding 15° and, in 90 % of the analyses, not exceeding 10°. The ChRM directions were extracted on orthogonal Zijderveld diagrams using 'free line fit' and in the case of the high-temperature components 'anchored line fit' methods (see Butler, 1992, pp. 121–2). The mean directions were calculated using Spheristat ver. 2.2 software employing a standard Fisher (1953) test. The ChRM directions were calculated from the site means. The site mean directions were obtained as an average of the independently oriented rock sample directions from a particular site, while every sample direction was the mean of its cylindrical specimen's directions derived from the PCA.

To calculate the ChRM components and describe relations between the ages of the identified ChRM

https://doi.org/10.1017/S0016756811000835 Published online by Cambridge University Press

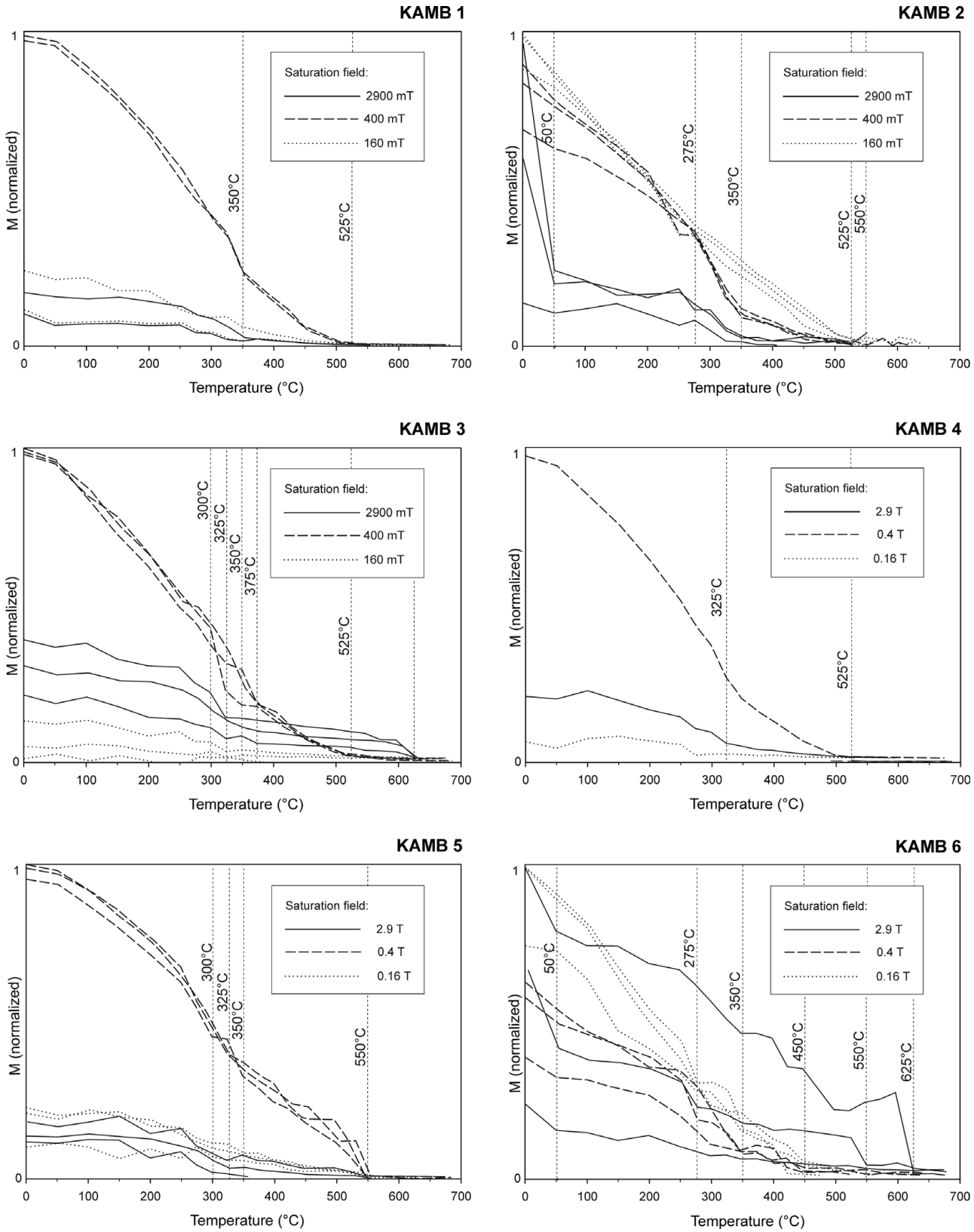

Figure 9. Results of three-component IRM acquisition curves (Lowrie, 1990) analyses conducted in particular palaeomagnetic sites of the Slaklidalen Formation. Changes of slope on demagnetization curves are marked by dotted lines and the temperatures of these points are given. Particular curves show demagnetization of different coercivity fractions existing in the samples: solid lines – ferromagnetic particles saturate between 400 mT and 2900 mT; dashed lines – those saturated between 160 mT and 400 mT; dotted lines – those saturated below 160 mT. M – normalized magnetization of the samples. The tests were performed on different numbers of samples in particular sites from 1 to 3.

https://doi.org/10.1017/S0016756811000835 Published online by Cambridge University Press

components and the stages of deformation in the sampled rocks, the inclination only test of Enkin & Watson (1996), using Enkin's (1994) program, was applied. Additionally, the graphs presenting the κ precision parameter of the population of the site means in particular stages of the unfolding procedure were plotted. A second procedure, which considers both declination and inclination parameters, was carried out using Spheristat (ver. 2.2) with a 10 % step of unfolding. The palaeopoles were calculated and compared with the APWP (apparent polar wander path) curves for Baltica and Laurentia using the GMAP 2002, 2003 software. The Baltica and Laurentia reference palaeopole paths and palaeointensity curves were compiled from Van der Voo (1993), Torsvik *et al*. (1996) and internal GMAP 2002, 2003 palaeopole libraries as well as the Early Palaeozoic palaeomagnetic data from Baltica of Torsvik & Rehnström (2001) and Lewandowski & Abrahamsen (2003).

4. Ferromagnetic minerals identification

Detailed optical and microprobe EDS observations have aided the identification of the ferromagnetic minerals and definition of their geometric relation with the host rock microstructures. From the oldest to the youngest the following generations (GEN) of the ferromagnetic minerals were recognized:

GEN. A. Consists of grains of magnetite lying in the foliated and recrystallized carbonate matrix. In thin-section (Fig. 6a) strings of iron ore grains (ferromagnetic grains?) can be seen to define clear intrafolial and sheared F_1–S_1 folds. It is not known whether these iron ore grains grew as primary (diagenetic?) phases or as a result of the pre- to syntectonic low-grade Caledonian metamorphism that is recorded in similar aged rocks throughout Western Svalbard (e.g. Ohta, 1979).

GEN. B. (Fe, Ti)-oxides and Fe sulphides, found in the tectonized and brecciated fragments of the limestones belong to this category (Fig. 6c). These ferromagnetic grains would have been subject to the same events as GEN A. The majority of Fe sulphides are framboidal pyrite with distinct Fe oxides or hydroxide aureoles.

GEN. C. These are grains of magnetite found within the calcite veins labelled KAMB KAL B cutting B generation grains (Fig. 6b). This generation of veins cuts the sheared S_1 foliation, which is seen on occasions to be affected by small-scale kink-like folds mentioned in Section 2 (Fig. 5). As noted above, the KAMB KAL B veins reflect a late S_1 extension phase which post-dates the kink folds. The ferromagnetic grains in these veins are interpreted to have precipitated at the same time as the calcite but the latter has subsequently recrystallized (Figs 5a, e, 6b).

The above observations strongly suggest that the ferromagnetic fabrics recorded in the Slaklidalen Formation limestones were imposed at different stages in the development of the S_1 foliation, and any primary depositional remanent magnetization (DRM) was overprinted by a secondary magnetization acquired during Caledonian times.

Unfortunately, the small size of the ferromagnetic grains (below 3 μm) observed in the polished sections prepared for microprobe studies excluded *in situ* WDS analyses. Grains large enough (size above 5 μm) for WDS composition determinations were found only in magnetic residuum of the dissolved limestones, so assignment of identified grains to particular microstructural elements was not possible. The results of WDS analyses are presented in Table 1. The ferromagnetic phases (Fig. 10) that were identified include haematite or maghaemite (5 grains), titanomagnetite (1 grain) and pyrrhotite (1 grain).

5. Rock magnetic experiments

Rock magnetic studies have revealed that the investigated Slaklidalen Formation contains a mixture of different ferromagnetic (*sensu lato*) phases. The majority of the SIRM decay curves possess the characteristics of titanomagnetite grains with maximum unblocking temperatures of about 540–550 °C (Kądziałko-Hofmokl & Kruczyk, 1976; Dunlop & Özdemir, 1997, pp. 61–7; Fig. 7). In one specimen (site KAMB 6) a higher maximum unblocking temperature range of 630–650 °C, close to the $T_{ub\,max}$ of haematite, was identified. In most specimens a notable change in the shape of SIRM curves was observed about points 330–350 °C (Fig. 7).

IRM acquisition curves reveal a dominance of a soft–medium coercivity fraction saturated in 0.2–0.4 T (Fig. 8). Some of the samples from sites KAMB 2, 3 and 6 do not, however, saturate in the maximum applied field of 2.9 T, suggesting an influence of high coercivity minerals (Fig. 8).

Thermal demagnetization curves of the three-component IRM acquisition experiments indicate that in most sites the medium coercivity fraction (0.12–0.4 T) dominates with distinct ranges of unblocking temperatures around 330–360 °C and 525–550 °C (Fig. 9). The points around 330–360 °C are close to the $T_{ub\,max}$ of pyrrhotite or maghaemite (Dunlop & Özdemir, 1997, pp. 66–9, 76–9). The appearance of the latter in the Slaklidalen Fm is suggested by Mössbauer investigations (Szlachta *et al*. 2008). Temperatures of 525–550 °C are close to the $T_{ub\,max}$ of the moderate to low Ti titanomagnetite (Dunlop & Özdemir, 1997, pp. 61–6). Soft (<0.12 T) and hard (>0.4 T) coercivity fractions play a more important role only in sites KAMB 2 and KAMB 6 (Fig. 9). In these locations the soft fraction curves imitate the shape of the medium curves and probably represent the same ferromagnetic minerals: pyrrhotite/maghaemite and titanomagnetite. The hard coercivity fraction curves of sites KAMB 2 and KAMB 6 record distinct unblocking temperatures of about 50 °C and 625 °C, which suggests significant increase of goethite and haematite (Dunlop & Özdemir, 1997, p. 51) in these locations.

https://doi.org/10.1017/S0016756811000835 Published online by Cambridge University Press

Table 1. Ferromagnetic minerals identified in the Slaklidalen Fm by WDS microprobe

	Sulphides				
	Sample				
	KBPT1	KBPT2	KBPT3	KBPT4	KBPT5
S	39.06	52.45	48.76	52.30	52.71
Cl	0.00	0.01	0.00	0.01	0.00
Cr	0.01	0.00	0.01	0.00	0.01
Fe	59.53	45.69	45.89	46.03	45.79
Co	0.03	0.07	0.03	0.00	0.00
Ni	0.00	0.06	0.14	0.00	0.00
As	0.00	0.03	0.00	0.04	0.01
SUM	98.63	98.31	94.84	98.37	98.53
Conversion	to 1 atom of S	to 2 atoms of S	to 2 atoms of S	to 2 atoms of S	to 2 atoms of S
S	1.000	2.000	2.000	2.000	2.000
Cl	0.000	0.000	0.000	0.000	0.000
Cr	0.000	0.000	0.000	0.000	0.000
Fe	0.859	0.983	1.062	0.993	0.980
Co	0.000	0.002	0.001	0.000	0.000
Ni	0.000	0.001	0.003	0.000	0.000
As	0.000	0.000	0.000	0.001	0.000
Interpretation	Pyrrhotite	Pyrite	Pyrite	Pyrite	Pyrite
Preparation	magnetic residuum	micro section	micro section	micro section	micro section

	Oxides					
	Sample					
	KBPT6	KBPT7	KBPT8	KBPT9	KBPT10	KBPT11
MgO	0.679	0.636	0.328	0.607	2.823	0.913
Al_2O_3					2.515	
SiO_2	0.221	0.287	0.155	0.195	0.131	0.126
CaO	0.019	0.03	0.021	0.04	0.078	0.071
TiO2	0.034	0.024	0.003	0.023	19.089	0.091
V_2O_3	0.047	0.066	0.076	0.045	0.517	0.025
Cr_20_3	0.052	0.041	0.043	0.048	1.156	0.782
MnO	0.218	0.237	0.094	0.331	0.715	0.131
FeO	89.698	89.214	90.900	90.863	67.612	87.819
NiO	–	0.415	–	–	0.151	–
ZnO	–	–	–	–	–	–
SUM	90.968	90.95	91.62	92.15181	94.787	89.958
Conversion	to 3 atoms of O	to 3 atoms of O	to 3 atoms of O	to 3 atoms of O	to 4 atoms of O	to 3 atoms of O
Mg	0.027	0.025	0.013	0.023	0.157	0.036
Al	0.000	0.000	0.000	0.000	0.111	0.000
Si	0.006	0.008	0.004	0.005	0.005	0.003
Ca	0.001	0.001	0.001	0.001	0.030	0.002
Ti	0.001	0.000	0.000	0.000	0.536	0.002
V	0.001	0.001	0.002	0.001	0.015	0.001
Cr	0.001	0.001	0.001	0.001	0.034	0.016
Mn	0.005	0.005	0.002	0.007	0.023	0.003
Fe^{2+}	0.000	0.000	0.000	0.000	1.354	0.000
Ni	0.000	0.009	0.000	0.000	0.005	0.000
Zn	0.000	0.000	0.000	0.000	0.000	0.000
Interpretation	Haematite/ maghaemite	Haematite/ maghaemite	Haematite/ maghaemite	Haematite/ maghaemite	Titanomagnetite	Haematite/ maghaemite
Preparation	magnetic residuum	magnetic residuum	magnetic residuum	magnetic residuum	magnetic residuum	magnetic residuum

Sample numbers correspond to those in Figure 10.

6. ChRM components

In 90 % of the Slaklidalen Formation specimens the NRM intensities were low and ranged between 0.2 and 0.5 mA/m. Only in the site KAMB 5 did they occasionally reach 3 mA/m.

The initial AF demagnetization of 18 specimens up to 40 mT did not resolve a consistent palaeomagnetic remanent magnetization direction. The thermal demagnetization was the most efficient method of extracting the NRM components. In the course of this treatment

https://doi.org/10.1017/S0016756811000835 Published online by Cambridge University Press

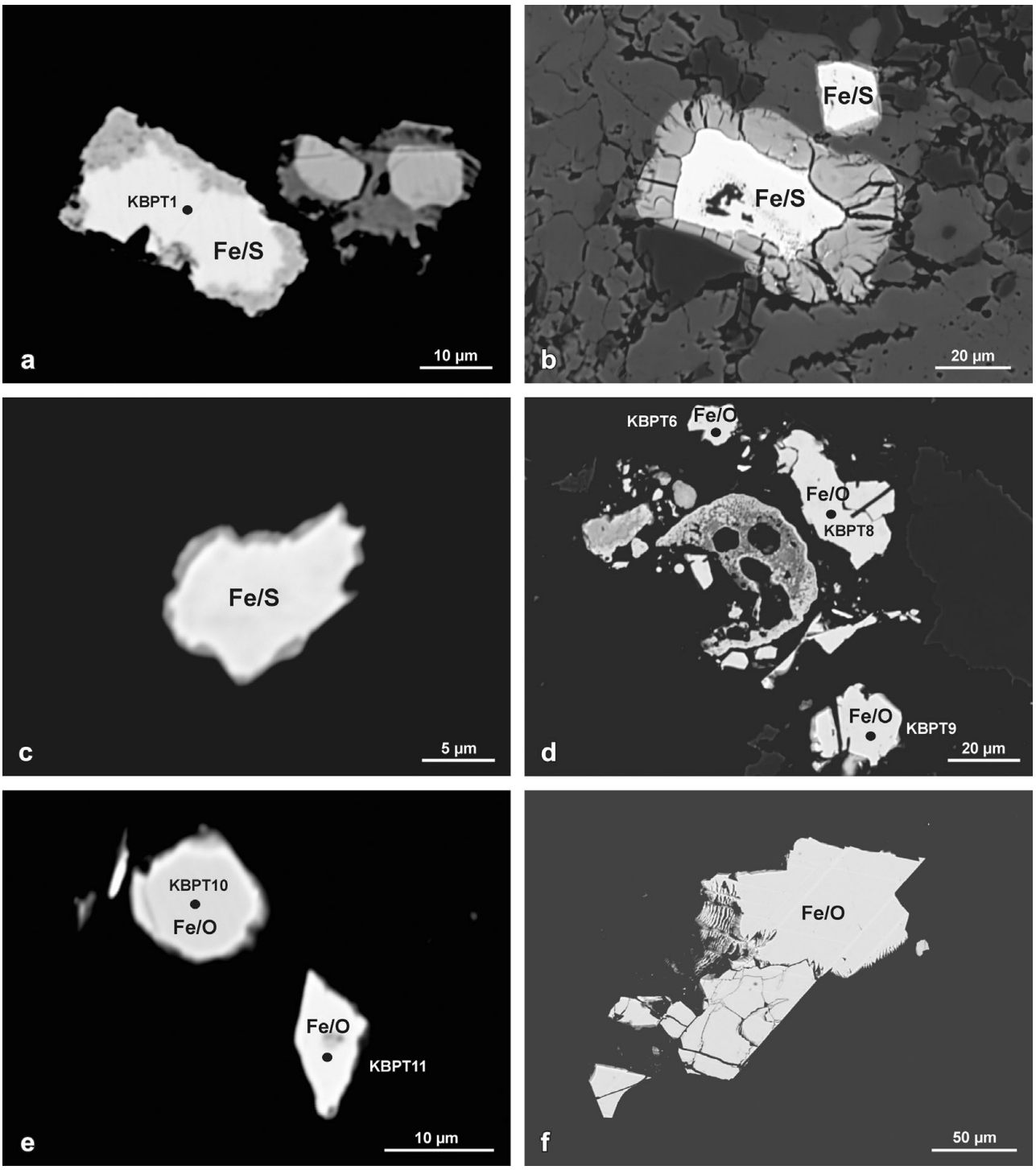

Figure 10. Identification of minerals with Fe content in Slaklidalen Fm samples; sample numbers on the grains correspond to the WDS analyses in Table 1. (a–c) Fe sulphides. (d–f) Fe oxides (a, c–f: magnetic residuum, b: thin-section; BSE microprobe images; chemical composition of selected grains has been defined by WDS analyses).

three ChRM directions were identified and, according to their unblocking temperatures, spectra in the low, middle and high ranges were labelled as the HORNL, HORNM and HORNH components, respectively. The parameters of the Fisher statistics of site means of particular ChRM directions are presented in Table 2.

In all sites samples revealed a similar demagnetization behaviour of NRM (Fig. 11). Up to 250 °C the HORNL soft component is demagnetized with variable declinations and very steep downward inclination that probably reflects the influence of the present-day magnetic field. Between 275–350 °C the HORNM component is identified in all six sites characterized by N- to NNE-directed declination and shallow downward inclination. Demagnetization of HORNM in the samples exhibits as much as an 80 % decrease in the intensity of their initial NRM signal. In five sites HORNM was extracted from Zijderveld diagrams

https://doi.org/10.1017/S0016756811000835 Published online by Cambridge University Press

Table 2. Statistical parameters of the ChRM means calculated from particular palaeomagnetic sites of the Sofiekammen syncline

Sites	Components	D (°)	I (°)	N/n	α95%	κ	Unblocking temperatures	ASD (°)
KAMB 1	HORN1L	268.8	70.7	6/16	8.5	63.37	50–275 °C	2.6–6.0
	HORN1M	3.6	23.9	6/15	4.3	241.8	275–340 °C	0.6–7.2
	HORN1H	5.4	29.9	5/9	5.8	174.0	360–450 °C	0.3–6.7
KAMB 2	HORN2L	324.8	71.8	8/12	12.2	18.89	50–200 °C	2.1–11
	HORN2M	20.8	16.6	8/15	5.6	97.29	275–340 °C	0.5 (0.0)–9.0
	HORN2H	–	–	–	–	–	–	–
KAMB 3	HORN3L	195.4	67.6	5/8	20.5	14.82	50–225 °C	2.8–9.0
	HORN3M	17.0	14.0	6/11	11.6	34.11	275–350 °C	2.3 (0.0)–9.6
	HORN3H	–	–	–	–	–	–	–
KAMB 4	HORN4L	214.5	73.8	7/12	26.6	6.114	50–250 °C	2.6–8.2
	HORN4M	16.9	0.1	7/13	15.9	15.59	275–340 °C	2.6–10.8
	HORN4H	344.5	24.9	4/4	57.1	3.569	360–450 °C	5.0–15.3
KAMB 5	HORN5L	114.2	73.1	6/11	18.3	14.31	50–200 °C	0.8–8.6
	HORN5M	21.0	4.5	7/17	6.6	84.04	275–340 °C	1.1 (0.0)–4.2
	HORN5H	32.1	−9.5	7/17	7.6	63.27	340–450 °C	2.9–11.5
KAMB 6	HORN6L	317.9	77.9	7/12	24.3	7.131	50–250 °C	2.4–5.8
	HORN6M	31.0	4.7	7/10	50.7	2.371	275–350 °C	0.5–9.7
	HORN6H	91.8	−59.3	3/3	30.1	17.87	350–400 °C	2.7–4.0

Abbreviations: D – declination, I – inclination, N – number of independently oriented hand samples, n – number of measured cylindrical specimens used for Fisher statistics, α95 % – half angle of a cone of 95 % confidence, κ – Fisherian precision parameter, ASD – angular standard deviation parameter describing precision of ChRM components definition on Zijderveld demagnetization diagrams.

Table 3. Results of palaeomagnetic fold tests

	ChRM parameters *in situ*				ChRM parameters after 100 % tectonic correction				
ChRM component	D	I	κ	α95 %	D	I	κ	α95 %	ChRM origin
HORNL	246	82	20.4	15.2	86.9	−39.2	1.515	90.2	Post-folding
HORNM	16.0	11.9	47.91	11.2	316.9	−22	3.847	45	Post-folding

ChRM component parameters have been presented for *in situ* position and after 100 % tectonic correction; other abbreviations are as in Table 2.

with high precision (in the majority of specimens ASD $<6^{\circ}$) and its mean directions, calculated at the level of palaeomagnetic sites, were very well defined with small 95 % confidence level cones and high precision parameters κ (Table 2). The mean HORNM of site KAMB 6 was an exception, which, with a high α95 % of 50.7 and a very low κ of 2.37, was thus rejected from further consideration.

The hard component HORNH was identified in the temperature range of 340–450 °C (Fig. 11). This component has been found in four palaeomagnetic sites and the site means were calculated with varying precision (Table 2). Two of the most precisely defined qualified for further analyses while the HORNH means of sites KAMB 4 (α95 % = 57.1, κ = 3.57) and KAMB 6 (α95 % = 30.1, κ = 17.87) were excluded.

In the course of the thermal demagnetization, the low-field magnetic susceptibility of the specimens was monitored. All specimens were characterized by a low initial susceptibility ranging from 10^{-4} to 10^{-5} SI. In most specimens there was no significant increase in susceptibility during their thermal cleaning (Fig. 12). In 30 % of specimens a substantial increase in susceptibility in the 450–500 °C range was noted. These temperatures were higher than the maximum unblocking temperatures of HORNH. The results of the susceptibility experiments suggest that possible chemical changes, which appeared during thermal demagnetization, did not disturb the original remanence directions in the Slaklidalen Formation.

7. Fold tests

The fold tests allowed determination of two ChRM directions (Graham, 1949; Cox & Doell, 1960). In these tests, statistical parameters for site mean vector distribution were calculated during stepwise unfolding until the Fisherian parameter κ reached its maximum (inclination only test; Enkin & Watson, 1996), or maximum κ and minimum α95 % was obtained using the test offered by the Spheristat software (ver. 2.2). The overall means for the best grouping direction were calculated and used for the purpose of a tectonic interpretation (Table 3).

The soft component HORNL showed the best statistical grouping before tectonic correction (Fig. 13):

(i) The inclination only test gave a maximum κ at 1.5 % of unfolding with a confidence level between −6.6 % and +11.1 % of unfolding;

(ii) The Spheristat (ver. 2.2) test gave a maximum κ = 20.4 and a minimum α95 % = 15.2° at 0 % of unfolding.

https://doi.org/10.1017/S0016756811000835 Published online by Cambridge University Press

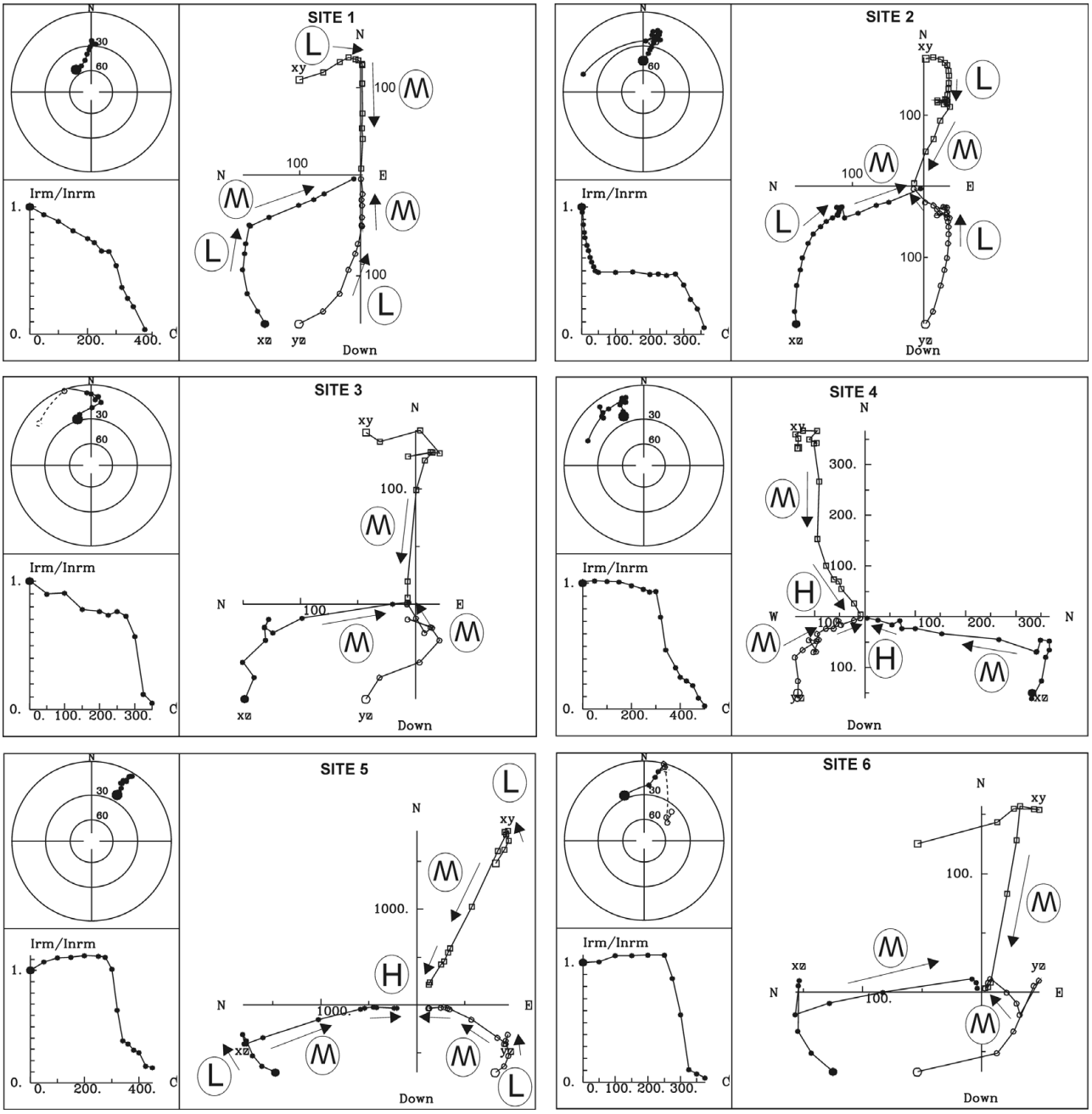

Figure 11. Equal area, orthogonal (Zijderveld) projections and normalized intensity decay plots of natural remanent magnetization of Slaklidalen Fm samples in the course of the thermal demagnetization process, representing all six palaeomagnetic sites situated in the Sofiekammen syncline; projections are presented for *in situ* orientation; open/full symbols represent upper/lower hemisphere; squares/circles denote projections onto horizontal/vertical planes; units on the orthogonal plots are in uA/m; ChRM components identified in particular specimens are marked on orthogonal projections by arrows with labels L, M, H representing HORNL, HORNM and HORNH directions, respectively.

The scatter of the HORNL on the stereogram is probably owing to a complex origin of this direction, which may be composed of at least two vectors.

The fold tests for the component HORNM show the following results (Fig. 14):

(i) The inclination only test gave a maximum κ at −2.1 % of unfolding with a confidence level between −8.4 % and 2.7 % of unfolding;

(ii) The Spheristat (ver. 2.2) test gave a maximum $\kappa = 47.91$ and a minimum $\alpha 95\,\% = 11.2^\circ$ at 0 % of unfolding.

As indicated by fold tests, both HORNL and the HORNM directions were acquired after folding. In terms of their quality, they pass the reliability criteria of Van der Voo (1993, p. 67; $N > 24$, $k \geq 10$ and $\alpha 95\,\% \leq 16^\circ$; Table 3).

For the purpose of the fold tests HORNH site means have been qualified from only two sites. As both sites are situated on the eastern limb of the Sofiekammen syncline, with similarly orientated beds, reliable fold tests for the HORNH component were not possible. However, HORNH site means have been presented

https://doi.org/10.1017/S0016756811000835 Published online by Cambridge University Press

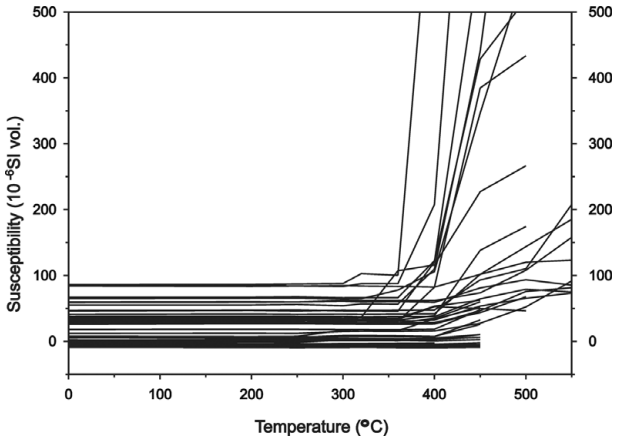

Figure 12. Changes of magnetic susceptibility of the 41 Slakidalen Fm specimens in the course of the thermal demagnetization process. Specimens represent all six palaeomagnetic sites sampled.

in stereograms in the *in situ* position, after 50 % and 100 % of unfolding (Fig. 15; Table 3). No overlap was found in any of the three positions. It should be noted, however, that in the *in situ* position HORNH site means are situated very close to the HORNM post-folding component (Fig. 14).

None of the sites passed the fold test. The post-folding development of the components identified in the Slaklidalen Formation reflects, therefore, a secondary magnetization and that any primary magnetization has been overprinted during syntectonic metamorphism responsible for the formation of the S_1 foliation.

8. Age of identified magnetic components and geotectonic implications

The ages of the HORNL, HORNM and HORNH components have been evaluated using APWPs of Baltica and Laurentia that were adjacent to Svalbard in Palaeozoic time (Figs 16, 17). The results have been compared with the isotopic record of the tectonothermal events of Hornsund (Birkenmajer, 1978, 1990; Manecki *et al*. 1998).

The Early Palaeozoic reference paths of Laurentia and Baltica differ significantly. While Laurentia was located in near-equatorial palaeolatitudes throughout Early Palaeozoic times, Baltica continued its drift away from the moderate southern palaeolatitudes it occupied in Cambrian time (Figs 16, 17). Following the Baltica–Laurentia collision, which is commonly attributed to the Scandian phase (*c*. 430 Ma), the two continents show overlapping drift histories from Late Silurian times. Here, the intention is to analyse the pre-Atlantic opening palaeogeography, and the Laurentian poles have been rotated to European coordinates around the Euler pole (lat. = 88°, long. = 27°) of Bullard, Everett & Smith (1965), by an angle of 38°, which has also been adopted in later reconstructions by Torsvik *et al*. (1996) and Torsvik & Rehnström (2001) for the Palaeozoic and Triassic sectors of APWPs. As none of the virtual geomagnetic poles (VGP) for the Laurentian Palaeozoic APWP came from Greenland, correction for the opening of the Labrador Sea was not made. Mesozoic and Cenozoic Baltica–Laurentia APWPs and palaeolatitude paths presented in this paper are based on the palaeomagnetic data from the European and North American plates derived from integral libraries of the GMAP 2002, 2003 software.

The $HORNL_{VGP}$ calculated for the low temperature HORNL component is distant from the APWPs of Baltica and Laurentia (Fig. 16; Table 4). To match the $HORNL_{VGP}$ with any sector of the reference paths a rotation of at least 150° is needed. A rotation of this magnitude would require thousands of kilometres of separation of West Spitsbergen from the European–North American regions in Phanerozoic time. Such a reconstruction is not supported by any up-to-date geological data, and this component is not considered to provide any meaningful palaeogeographic information.

The HORNL direction probably represents a composite vector as the low temperature NRM record up to 250 °C is particularly prone to re-magnetization. The high inclination parameter (Figs 11, 13; Tables 2, 3, 4) suggests a strong influence of the recent geomagnetic field.

The $HORNM_{VGP}$ calculated from the post-folding HORNM component matches exactly the Silurian sector of the Baltica–Laurentia APWPs, the first common part of the reference paths of the two continents occurring after the closure of Iapetus (Figs 16, 17). The $HORNM_{VGP}$ D_p/D_m oval overlaps the Baltica palaeopoles around 428–420 Ma derived from Gotland and southern Norway (Claesson, 1979; Douglass, 1988; Trench & Torsvik, 1991). Simultaneously, the $HORNM_{VGP}$ exactly matches the 420 Ma Laurentian

Table 4. Palaeopoles (southern) calculated from ChRM components identified in the Slaklidalen Formation, Hornsund area, southern Spitsbergen (average location of Slakidalen palaeomagnetic sites 77° 00′ N, 15° 50′ E)

VGP Symbol	N	n	S	P	D (°)	I (°)	α95 % (°)	κ	Φ (°) N	Λ (°) E	D_p/D_m (°)	Plat (°)	Genesis of ChRM
$HORNL_{VGP}$	39	71	6	N	246	82	15.2	20.4	−66.0	158.4	28.7/29.6	74	Post-folding
$HORNM_{VGP}$	34	71	5	N	16	11.9	11.2	47.91	−18.5	359	5.8/11.4	6	Post-folding
$HORN1H_{VGP}$	5	9	1	N	5.4	29.9	5.8	174	−29	9.9	3.6/6.4	16	?
$HORN5H_{VGP}$	7	17	1	R	32.1	−9.5	7.6	63.27	−6.2	343.6	3.9/7.7	4.8	?

Abbreviations: S – number of sites from which the ChRM was calculated; P – polarity; Φ – palaeopole latitude; Λ – palaeopole longitude; D_p/D_m – half axes of palaeopole oval of 95 % confidence limit; Plat – palaeolatitude; other abbreviations are as in Table 2. $HORNH1_{VGP}$ and $HORNH5_{VGP}$ have been calculated from the site means not from the results of the fold test (for explanation see Sections 7 and 8).

https://doi.org/10.1017/S0016756811000835 Published online by Cambridge University Press

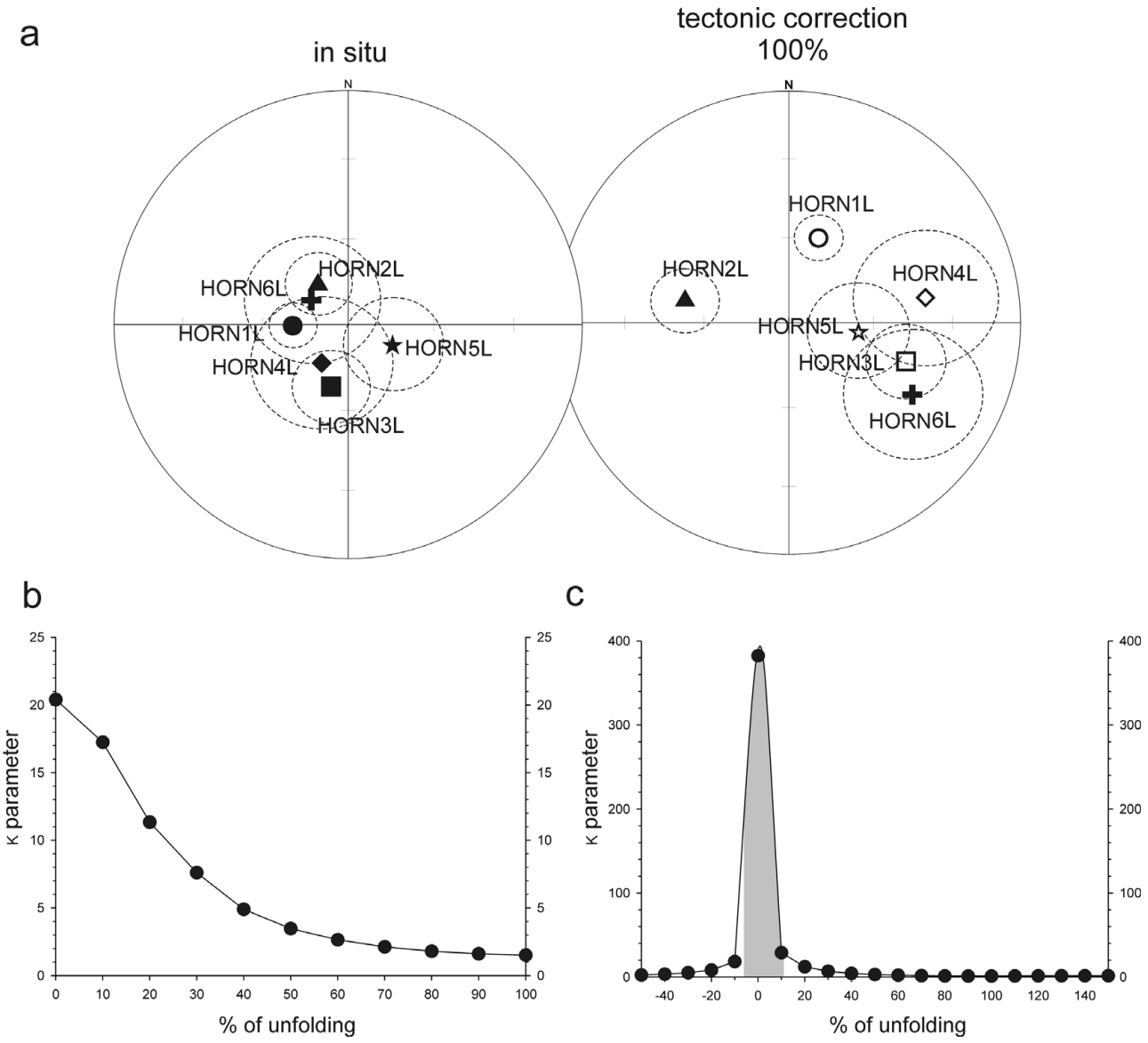

Figure 13. (a) Equal area projections of HORNL site means in *in situ* and after 100 % tectonic correction positions; open/full symbols represent upper/lower hemisphere, site means are presented with their cones of α95 % confidence. (b) Graph presenting changes of the κ precision parameter of the population of the HORNL site means in the course of the unfolding procedure. (c) Inclination only test for HORNL site means according to the procedure of Enkin & Watson (1996); the grey bar represents 95 % confidence level.

VGP of the Scottish Peterhead granite (Torsvik, 1985) and it also overlaps the 455–415 Ma Laurentia VGPs derived from Scotland, Newfoundland and Indiana, USA (Hodych, 1989; Hall & Evans, 1988; Deutsch & Prasad, 1987; Torsvik, 1984; McCabe *et al*. 1985; Turnell, 1985). The close fit of $HORNM_{VGP}$ with the 455–415 Ma sectors of the two APWPs coincides in time with the 432 ± 7 Ma ^{40}Ar–^{39}Ar age obtained by Manecki *et al*. (1998) from the adjacent Proterozoic Sofiebogen Group, which is interpreted as recording the timing of the syntectonic (D_1–F_1–S_1) Caledonian greenschist-facies metamorphism in the Hornsund region.

This exceptional fit would argue against any large-scale movements between SW Spitsbergen, Laurentia and Baltica after 455 Ma. Moreover, the clearly post-folding origin of the HORNM component implies (Fig. 14) that the geometry of Sofiekammen fold has not been significantly modified by the Svalbardian or the WSFB events, (cf. also Birkenmajer, 1990). It is evident, therefore, that the Sofiekammen syncline, its S_1 foliation and related shearing fabrics are entirely Caledonian in origin.

In the majority of the investigated sites the small number of reliable palaeomagnetic directions demagnetized above 340 °C prevented determination of the hard component HORNH. The HORNH site means with acceptable κ, and α95 % Fisher parameters have been obtained, however, from two sites: KAMB 1 and KAMB 5 (Table 2). Although they are statistically distant from the HORNM site means (Figs 14, 15; Table 2), the $HORNH_{VGP}$ (Figs 16, 17; Table 4) does lie in the vicinity of the $HORNM_{VGP}$. This coincidence may suggest that at least two pulses of magnetization

https://doi.org/10.1017/S0016756811000835 Published online by Cambridge University Press

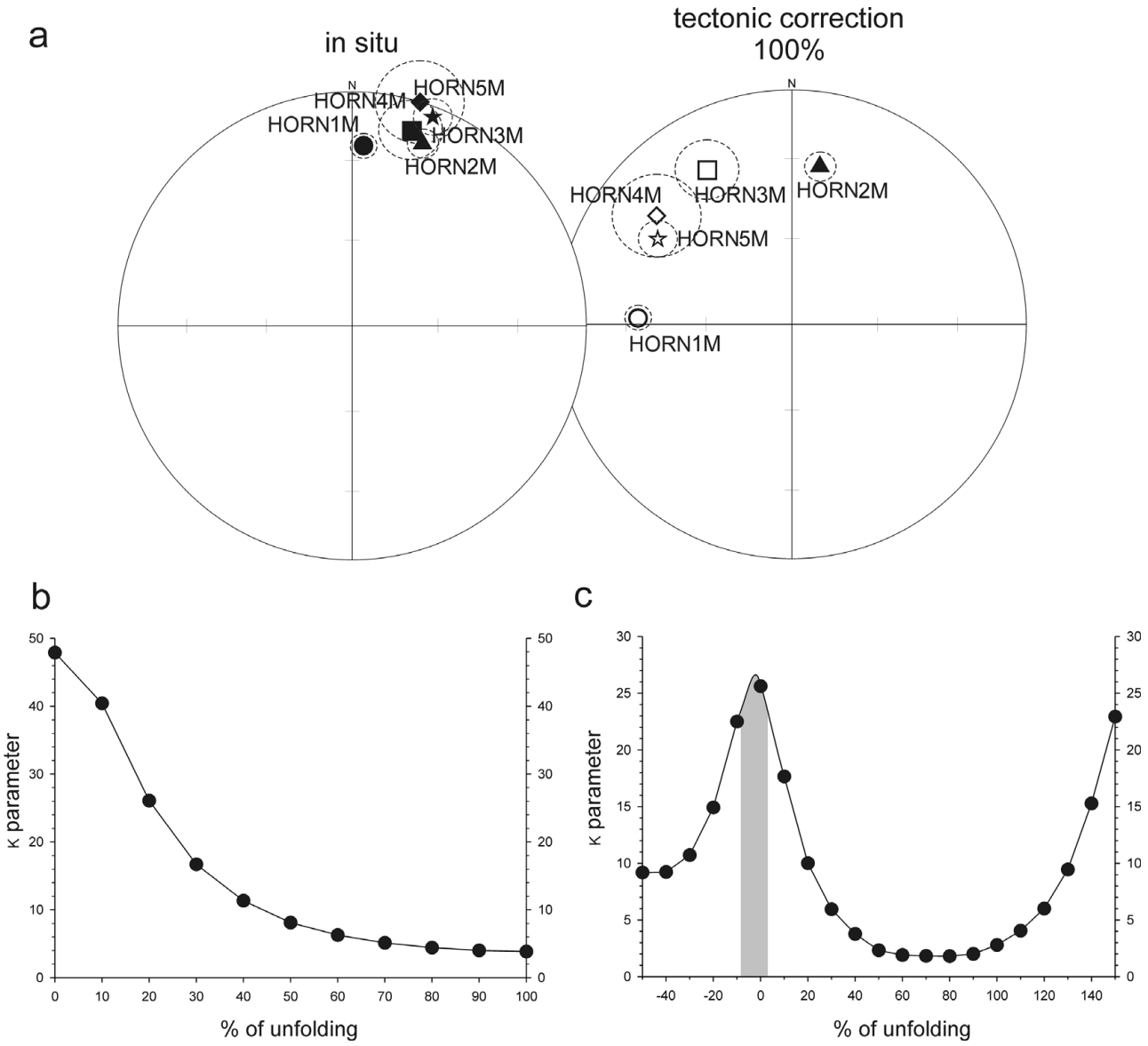

Figure 14. (a) Equal area projections of HORNM site means in *in situ* and after 100 % tectonic correction positions. (b) Graph presenting changes of the κ precision parameter of the population of the HORNM site means in the course of the unfolding procedure. (c) Inclination only test for HORNM site means according to the procedure of Enkin & Watson (1996); other explanations as in Figure 13.

occurred during Caledonian tectogenesis. The above mineral-fabric relations demonstrate that these magnetization events occurred before the final development of the S_1 foliation.

Since the palaeomagnetic age of the HORNM and HORNH components coincides with the *c*. 432 Ma age for the greenschist-facies metamorphism determined on the basis of ^{40}Ar–^{39}Ar dating by Manecki *et al*. (1998), these components are interpreted to be the result of the Caledonian thermal magnetization, acquired during the syntectonic metamorphism, subsequent exhumation and cooling.

9. Central and Eastern terranes relations

New ^{40}Ar–^{39}Ar dating results from mylonites developed along the BFZ in Ny Friesland are presented here, which shed new light on the spatial relationships of the Central and Eastern terranes in the Silurian–Devonian interval. To better determine the possible relative geographical positions of the Caledonian terranes of Svalbard in Early Palaeozoic time, palaeomagnetic data from pre-Devonian rock formations from different parts of the Svalbard Archipelago are needed. Currently, the only other published palaeomagnetic data concerning the pre-Devonian rocks of Svalbard are that of Maloof *et al*. (2006), which are concerned with the Neoproterozoic rocks of Ny Friesland (Eastern Terrane). The palaeomagnetic results of Maloof *et al*. (2006) from the Eastern Terrane are discussed in the light of the Caledonian re-magnetization of the Cambrian Slaklidalen Fm rocks of Hornsund (SW Terrane). To further this discussion, however, some consideration of the Caledonian deformation and metamorphism that has affected the Eastern Terrane (Ny Friesland) is needed.

https://doi.org/10.1017/S0016756811000835 Published online by Cambridge University Press

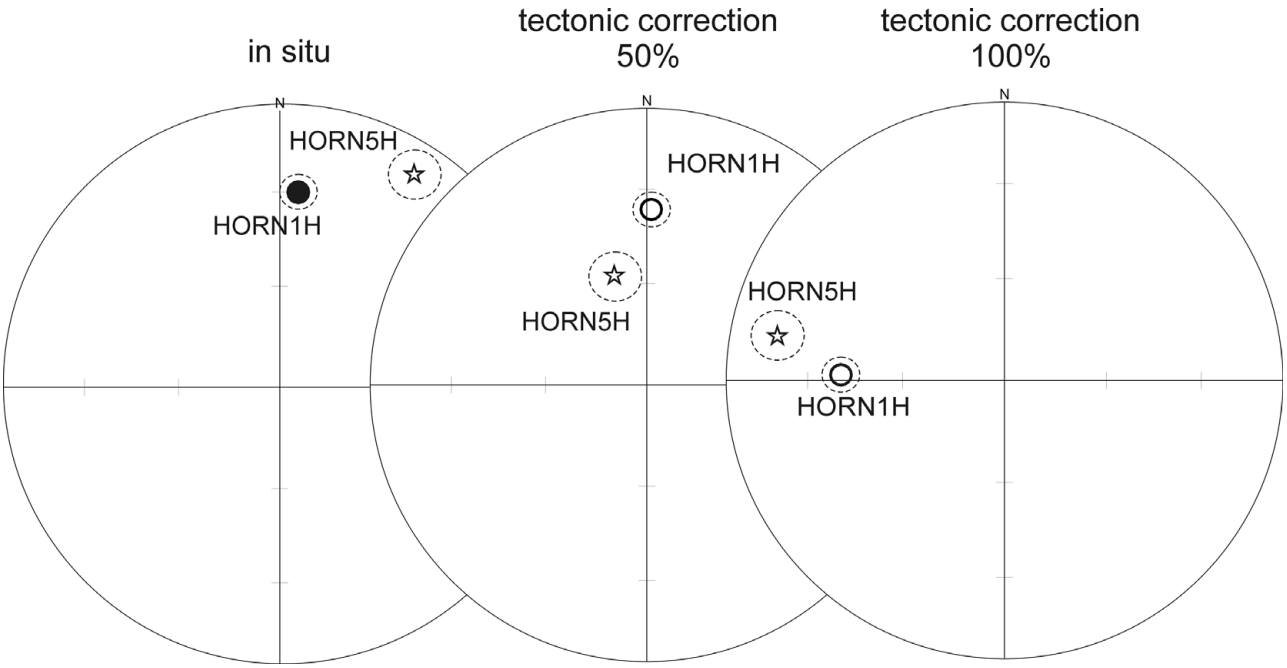

Figure 15. (a) Equal area projections of HORNH site means in *in situ*, after 50 % and after 100 % tectonic correction positions; other explanations as in Figure 13.

It is widely accepted that the N–S-trending BFZ, which forms the boundary between the Eastern and Central terranes of Svalbard (Harland & Wright, 1979), also constitutes the eastern border of the Devonian Basin of Northern Svalbard (e.g. Manby & Lyberis, 1992; Manby *et al*. 1994). While no large-scale Devonian Basin controlling brittle fault is exposed onshore in Ny Friesland a number of N–S-trending, W-dipping, small-scale (of limited throw and lateral extent) faults are noticeable along the west coast of Ny Friesland. In Central Svalbard, however, larger expressions of the BFZ can be observed to juxtapose the Devonian–Carboniferous rocks and the sheared high-grade gneisses (see Harland, 1997). Along the western margin of Ny Friesland the high-grade gneisses are retrograded to greenschist-facies assemblages over a 2–3 km wide zone with abundant microstructures demonstrating sinistral and E-vergent shear (cf. Manby, 1990; fig. 6a, b in Lyberis & Manby, 1999). This shear zone is taken here to represent the deeper ductile component of the BFZ which facilitated the assembly of the Eastern and Central terranes. The timing of these movements is controversial but recently acquired ^{40}Ar–^{39}Ar ages obtained from various white mica fractions separated from quartz-mica mylonites within the ductile shear zone give an average age of 450 Ma (Table 5), suggesting that significant ductile deformation ceased at this time along the BFZ. Nevertheless, this fault zone was active as a brittle structure during the filling of the Devonian Basin and its subsequent inversion (Manby & Lyberis, 1992; Manby *et al*. 1994). Seismic reflection profiles across the northern offshore margin of Svalbard show that the BFZ can be traced several kilometres offshore, north of the mainland (Eiken & Austegard, 1987), where it is seen as a W-dipping extensional structure displacing undeformed post-Devonian sediments. The displacement of these rocks along the BFZ may have been the product of the post-Eocene extension of the western margin of Svalbard during the accretion of the Knipovitch Ridge (Eiken & Austegard, 1987). The preservation of the 450 Ma ^{40}Ar–^{39}Ar ages from the ductile shear zone suggests that the later brittle movements were either located offshore or that their effects were so localized they did not disturb the isotope systematics in the sampled mylonites.

In the context of the effects of the Caledonian events it is notable that the Mid-Proterozoic Veteranen and Akademikerbreen (cf. Harland, 1997) rocks of eastern Ny Friesland (the Eastern Terrane) described by Maloof *et al*. (2006) are affected by large-scale, fault propagation, periclinal (D_1/F_1) folds with strong cleavage (S_1) development in pelitic rocks. Low-grade regional metamorphism has accompanied this deformation with chlorite and/or biotite often seen as early to syntectonic phases lying in the S_1 foliation in pelitic rocks. Other Veteranen Group (Harland, 1997) pelites to the northwest of one of their (Raudberget) study areas, for example, are characterized by the presence of a regional metamorphic, early to pre-tectonic (with respect to the D_1 deformation) biotite. A later contact metamorphic overprint, imposed by the intrusion of the Late Orogenic Chydeniusbreen Granite (Lyberis & Manby, 1999), followed the development of the D_2 crenulation folding (cf. Fig. 18). The presence of early tectonic (Caledonian) biotite has also been observed (by G. M. Manby) in some of the semipelitic rocks associated with the tillite-bearing Polarisbreen Group rocks collected from the Backlundtoppen area by Hambrey (1982). To the west of their (Maloof

https://doi.org/10.1017/S0016756811000835 Published online by Cambridge University Press

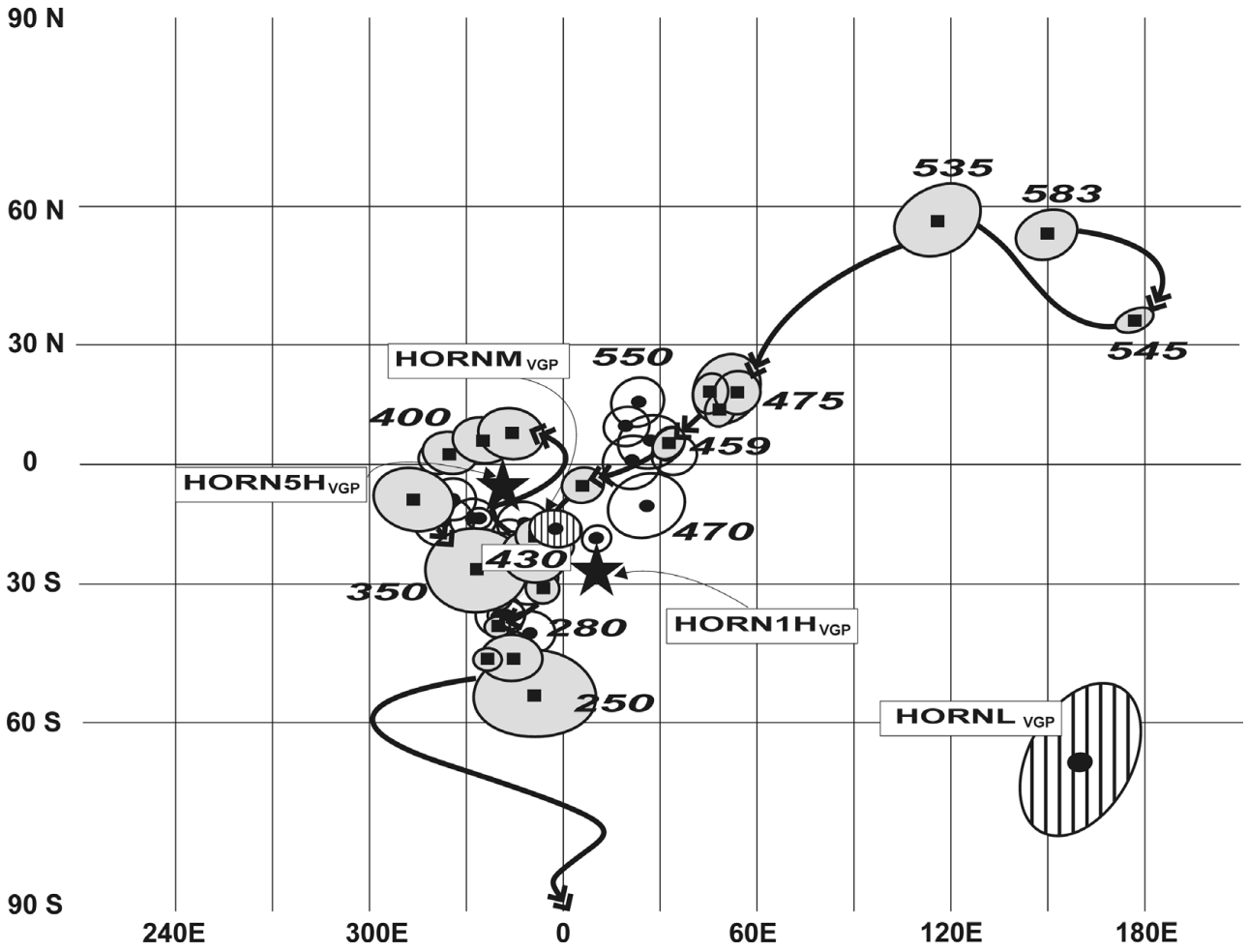

Figure 16. The positions of palaeopoles obtained from the Cambrian Slaklidalen Fm relative to the APWPs of Baltica and Laurentia; palaeopoles of Baltica (grey ovals) and Laurentia (white ovals) are presented with their D_p/D_m ovals of 95 % confidence; the age of the sectors of reference paths is given; palaeopoles for Baltica and Laurentia have been selected from Van der Voo (1993), Torsvik *et al*. (1996), internal GMAP 2002, 2003 palaeopole libraries and additional Early Palaeozoic palaeomagnetic data from Baltica from Torsvik & Rehnström (2001) and Lewandowski & Abrahamsen (2003); $HORNM_{VGP}$ and $HORNL_{VGP}$ palaeopoles (striped ovals) are presented with their D_p/D_m ovals of 95 % confidence; the positions of $HORN1H_{VGP}$ and $HORN5H_{VGP}$ palaeopoles are marked by black stars.

et al. 2006) study area, the Middle Proterozoic succession (Lomfjorden Super Group, Harland, 1997) of Eastern Svalbard is juxtaposed against the high-grade schists and gneisses of the Early Proterozoic (Studendorfbreen Super Group, Harland, 1997) of Ny Friesland. The relationship between these two successions is controversial, with some authors (e.g. Harland, 1997) suggesting that the entire succession is effectively continuous. Others, however, (Manby, 1990; Lyberis & Manby, 1999) have drawn attention to the presence of a wide mylonite zone (Eolussletta Shear Zone, Fig. 2) separating the two successions. In northern Ny Friesland this shear zone is steeply inclined with numerous sinistral kinematic indicators (see Lyberis & Manby, 1999, fig. 6) while in Central Ny Friesland (G. M. Manby, unpub. data) the younger and lower greenschist-facies rocks to the east are overthrust from the west by the upper amphibolite-facies schists and gneisses. Whatever the initial relations of these two rock sequences were, it is clear that the Caledonian events have assembled them into a single tectonic unit.

To confirm the unity of these two successions and the amalgamation of the Eastern and Central terranes by 450 Ma, the Caledonian palaeomagnetic record together with supporting isotopic age determinations from the various blocks are needed.

Despite the above observations concerning the expressions of Caledonian metamorphism and deformation in Ny Friesland, Maloof *et al*. (2006) maintain that there is no sign of Caledonian re-magnetization within their investigated rocks and all three high-temperature components recognized in three sampled formations are primary. Taking into account the results from Hornsund and after careful recalculation of the data presented by Maloof *et al*. (2006), we suggest that their lGfm ChRM derived from the Middle Proterozoic Lower Grusdievbreen Fm (lGfm) of the Ny Friesland Eastern Terrane (NFET of Harland, 1997), which they interpret to be primary, may equally be a product of Caledonian re-magnetization. The $lGfm_{VGP}$ of Maloof *et al*. (2006) lies close to $HORNM_{VGP}$ ($\Phi = -18.5^\circ$, $\Lambda = 359^\circ$, $D_p/D_m = 5.8^\circ/11.4^\circ$, Plat = 6°; Fig. 17).

https://doi.org/10.1017/S0016756811000835 Published online by Cambridge University Press

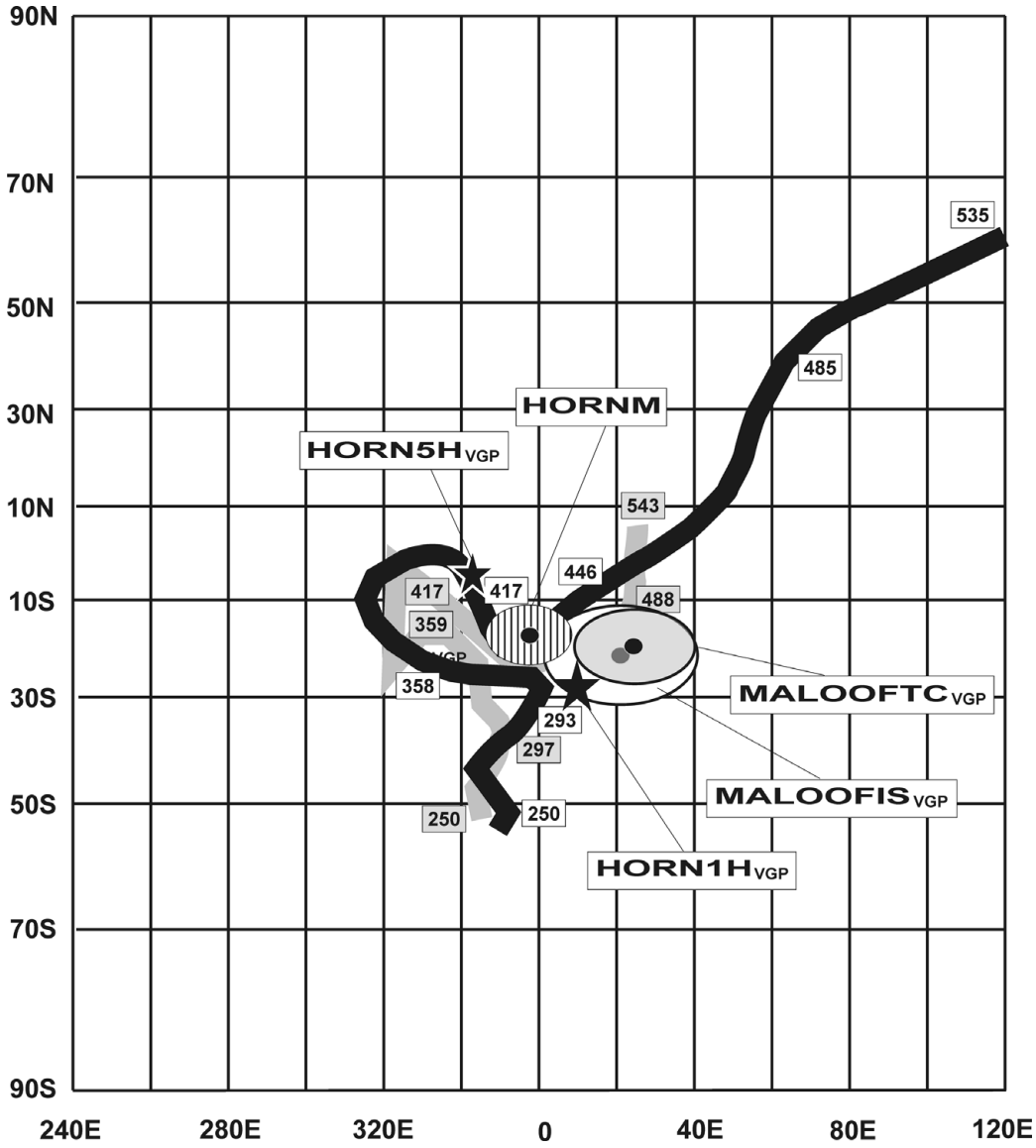

Figure 17. The relative positions of palaeopoles obtained from Central Svalbard Terranes (Hornsund Terrane, this study) and Eastern Svalbard Terranes (Maloof *et al*. 2006; division of Svalbard into geotectonic provinces after Harland, 1997) to the reference paths of Baltica (black) and Laurentia (grey) mathematically smoothed by the spline method (paths of Baltica and Laurentia are taken from internal GMAP 2002, 2003 libraries). Abbreviations: $MALOOFTC_{VGP}$ – tectonically corrected Lower Grusdievbreen Fm palaeopole of Maloof *et al*. (2006); $MALOOFIS_{VGP}$ – Lower Grusdievbreen Fm palaeopole of Maloof *et al*. (2006) in *in situ* position; other abbreviations are as in Figure 16.

None of the tests derived by Maloof *et al*. (2006) prove, unequivocally, the primary character of the lGfmVGP. Their lGfm ChRM is generally sub-parallel to the strike of regional folds (Maloof *et al*. 2006), and tectonic corrections applied by Maloof *et al*. (2006) do not change, significantly, its direction. The mean directions of the lGfm component calculated on the level of the sections before and after 100 % tectonic correction fall within the α95 % circles of each other and are not distinct at the 5 % significance level (see Maloof *et al*. 2006, their table 1). The fit of our $HORNM_{VGP}$ with their lGfmVGP is improved further if the Grusdievbreen Fm ChRM is regarded as post-folding secondary magnetic overprint and if its VGP is recalculated for the lGfm *in situ* position, without any tectonic correction (D = 357.9° E, I = 19.2° N, α95 % = 18.8°, Φ = −20.4°, Λ = 20.4°, D_p/D_m = 10.2°/19.6°, Plat = 9.9°; Fig. 17). For this recalculation the average location, 79° 27′ N, 18° 12′ E, of the Maloof *et al*. (2006) sampling sites (see their table 1) was used here. The McFadden & McElhinny (1990) reversal tests are also inconclusive for the lGfm because the collection of the samples with reversed polarity recognized in the sampled sections is too small (Maloof *et al*. 2006). They may equally be a product of selective demagnetization during another pulse of the Caledonian magnetic event.

It would appear that the widespread low-grade metamorphism exhibited by rocks of pelitic composition in eastern Ny Friesland has not been given due consideration by Maloof *et al*. (2006). Consequently, their general conclusion, that the region was not

https://doi.org/10.1017/S0016756811000835 Published online by Cambridge University Press

Table 5. $^{40}Ar/^{39}Ar$ analyses of hand picked muscovite fractions extracted from the Billefjorden Fault Zone quartz-mica mylonites of Western Ny Friesland (analyses performed at the Open University, UK)

Sample	^{40}Ar	±	^{39}Ar	±	^{38}Ar	±	^{37}Ar	±	^{36}Ar	±	$^{40}Ar^*/^{39}Ar$	±	Age (Ma)	±
G90-2	0.2339	4.5E-04	9.4E-03	1.0E-05	1.3E-04	0.0E+00	2.2E-03	5.4E-04	2.5E-05	5.0E-06	24.0066	0.1656	449	4
G90-2	0.4400	3.5E-04	1.8E-02	1.0E-05	2.4E-04	1.0E-05	2.2E-03	6.9E-04	1.0E-05	0.0E+00	24.3061	0.0238	454	1
G90-2	0.3559	2.1E-04	1.5E-02	3.1E-05	2.0E-04	1.0E-05	2.1E-03	3.8E-04	0.0E+00	1.0E-05	24.3787	0.2094	455	4
G90-2	0.6152	3.7E-04	2.5E-02	2.1E-05	3.6E-04	1.0E-05	4.3E-03	4.6E-04	0.0E+00	0.0E+00	24.1777	0.0244	452	1
G90-2	0.6207	3.2E-04	2.6E-02	2.1E-05	3.4E-04	1.0E-05	6.8E-03	2.3E-04	1.5E-05	5.0E-06	23.9482	0.0618	448	1
G90-2	1.5751	6.3E-03	6.5E-02	2.5E-04	8.7E-04	1.1E-05	2.0E-02	1.3E-03	6.0E-05	1.0E-05	23.8871	0.1401	447	3
G90-2	0.9149	1.4E-03	3.8E-02	1.2E-04	5.0E-04	5.1E-06	1.2E-02	3.8E-04	7.5E-05	5.0E-06	23.2405	0.0921	436	2
G90-2	0.9922	1.3E-03	4.1E-02	6.3E-05	5.3E-04	5.1E-06	8.9E-03	2.0E-03	5.0E-06	5.0E-06	23.8801	0.0601	447	1
G90-2	1.0935	1.9E-03	4.5E-02	5.2E-05	5.8E-04	0.0E+00	1.4E-02	1.2E-03	5.0E-05	0.0E+00	24.0318	0.0511	449	1
G90-2	1.1841	1.6E-03	4.8E-02	6.2E-05	5.8E-04	1.0E-05	1.4E-02	2.3E-04	9.0E-05	1.0E-05	23.8735	0.0755	447	2
G90-2	0.6040	3.0E-04	2.4E-02	2.1E-05	2.9E-04	5.1E-06	3.4E-03	1.5E-03	2.5E-05	5.0E-06	24.6675	0.0658	460	1
G90-2	0.8712	8.8E-04	3.6E-02	5.2E-05	4.7E-04	5.1E-06	1.1E-02	7.8E-04	4.5E-05	1.5E-05	23.7995	0.1299	445	3
G90-2	1.1749	9.4E-04	4.9E-02	6.2E-05	6.1E-04	5.1E-06	7.1E-03	2.3E-04	5.0E-06	5.0E-06	23.9647	0.0468	448	1
G90-2	0.6391	3.0E-04	2.7E-02	2.1E-05	3.3E-04	0.0E+00	3.4E-03	6.3E-04	5.0E-06	5.0E-06	23.8778	0.0595	447	1
G90-2	0.6621	3.7E-04	2.8E-02	2.1E-05	3.6E-04	5.1E-06	4.2E-03	6.3E-04	2.5E-05	1.5E-05	23.7791	0.1625	445	3
G90-2	0.9337	5.0E-04	3.9E-02	3.1E-05	4.7E-04	1.1E-05	5.4E-03	3.9E-04	2.0E-05	1.0E-05	24.3409	0.0801	454	2
McM39	0.5050	6.0E-04	2.1E-02	2.1E-05	2.9E-04	5.1E-06	3.0E-03	1.4E-03	1.0E-05	1.0E-05	24.2222	0.1475	452	3
McM39	0.6611	5.9E-04	2.8E-02	3.1E-05	3.5E-04	5.1E-06	4.2E-03	1.4E-03	3.0E-05	1.0E-05	23.6985	0.1128	444	2
McM39	1.1971	1.8E-03	5.0E-02	8.3E-05	6.5E-04	5.1E-06	9.8E-03	1.5E-03	2.0E-05	1.0E-05	23.6263	0.0790	443	2
McM39	0.7596	4.5E-04	3.1E-02	2.1E-05	3.9E-04	5.1E-06	8.9E-03	1.5E-03	2.0E-05	1.0E-05	24.2167	0.0974	452	2
McM39	0.9570	5.4E-04	4.0E-02	3.1E-05	4.8E-04	0.0E+00	6.8E-03	4.4E-04	1.5E-05	1.5E-05	23.9854	0.1140	448	2
McM39	0.5389	1.5E-04	2.2E-02	2.1E-05	2.7E-04	0.0E+00	7.1E-03	4.4E-04	5.5E-05	1.5E-05	24.0380	0.2053	449	4
McM39	0.7482	1.9E-04	2.9E-02	3.1E-05	3.6E-04	5.1E-06	5.8E-03	0.0E+00	3.5E-05	2.5E-05	25.1573	0.2534	468	5
McM39	0.8057	4.8E-04	3.3E-02	3.1E-05	4.4E-04	1.0E-05	4.1E-03	8.8E-04	1.0E-05	2.0E-05	24.0248	0.1788	449	4
McM39	0.8733	4.0E-04	3.6E-02	2.1E-05	4.3E-04	1.0E-05	4.0E-03	7.9E-04	2.0E-05	2.0E-05	24.0107	0.1646	449	3
McM39	0.8489	4.7E-04	3.5E-02	4.1E-05	4.5E-04	0.0E+00	4.7E-03	2.6E-04	1.0E-05	2.0E-05	24.0165	0.1707	449	4
McM39	1.0622	3.5E-04	4.4E-02	2.1E-05	5.5E-04	5.1E-06	6.4E-03	3.5E-04	5.0E-05	2.0E-05	23.6669	0.1342	443	3
McM39	1.0599	3.9E-04	4.4E-02	3.1E-05	5.5E-04	0.0E+00	8.3E-03	1.8E-04	6.5E-05	1.5E-05	23.8369	0.1033	446	2

Statistical Mean Age = 450.6 ± 1.6 Ma (0.36 %) 95 % confidence. Weighted by data point errors only, 0 of 28 rejected. Mean Square Weighted Deviation = 9.2, probability = 0.000.

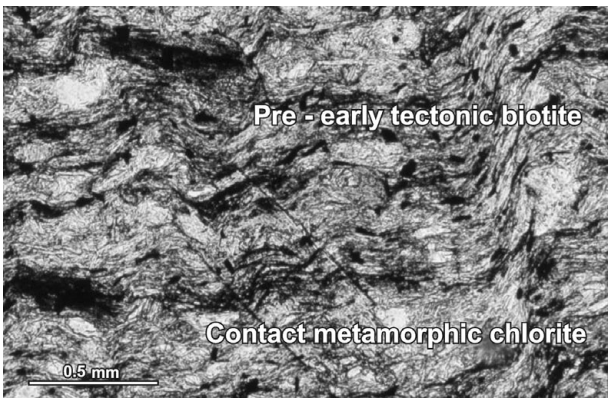

Figure 18. Thin-section of a semi-pelite from the Lower Veteranen Group, south Glasgowbreen, Ny Friesland. This shows a pre-early S_1 biotite wrapped by the S_1 foliation with small pressure shadows. The larger almost transparent chlorite that overgrows the S_1 foliation and the later crenulation folds is a contact metamorphic phase related to the intrusion of the Chydenius Granite a few kilometres to the east.

affected by any significant thermal or deformation events in the Late Proterozoic–Silurian interval, is questionable.

The position of the $HORNM_{VGP}$ on the Baltica–Laurentia reference paths together with the lack of significant post 450 Ma lateral displacement along the BFZ that separates the two terranes provides convincing evidence for their amalgamation by Late Silurian time. The similarity of the palaeolatitudes in which the HORNM and the lGfm (Fig. 19) components were magnetized, together with the overlap of the VGP ovals from the Central and Eastern terranes (Fig. 17) suggests that both were subjected to the metamorphically induced Caledonian re-magnetization event.

10. Conclusions

In conclusion it should be stressed that although our palaeomagnetic results from the Cambrian Slaklidalen Fm of Hornsund generally stabilize the position of Svalbard relative to Laurentia and Baltica from Late Silurian time, Late Palaeozoic, Mesozoic and Cenozoic crustal movements in the target area cannot be completely excluded. The Silurian VGP from Hornsund was obtained with defined precision, which in this particular case can be assessed to within $\pm 6^\circ$ along the meridian and $\pm 11.5^\circ$ along the parallel (Figs 16, 17, 19; Table 4). Precise reconstructions of Svalbard's pre-Caledonian terranes relative to their proposed counterparts in East and Northeast Greenland are not yet possible, primarily because reliable palaeomagnetic data from the latter areas are lacking. Further, the Palaeozoic to Mesozoic positions of Greenland relative to North America are imprecisely known. The uncertainty in any Palaeozoic reconstructions of the Arctic Caledonides is added to by the unknown scale of the crustal extension that occurred across the Barents and Northeast Greenland shelves during the opening of the North Atlantic and Arctic Ocean basins (Mosar *et al*. 2002).

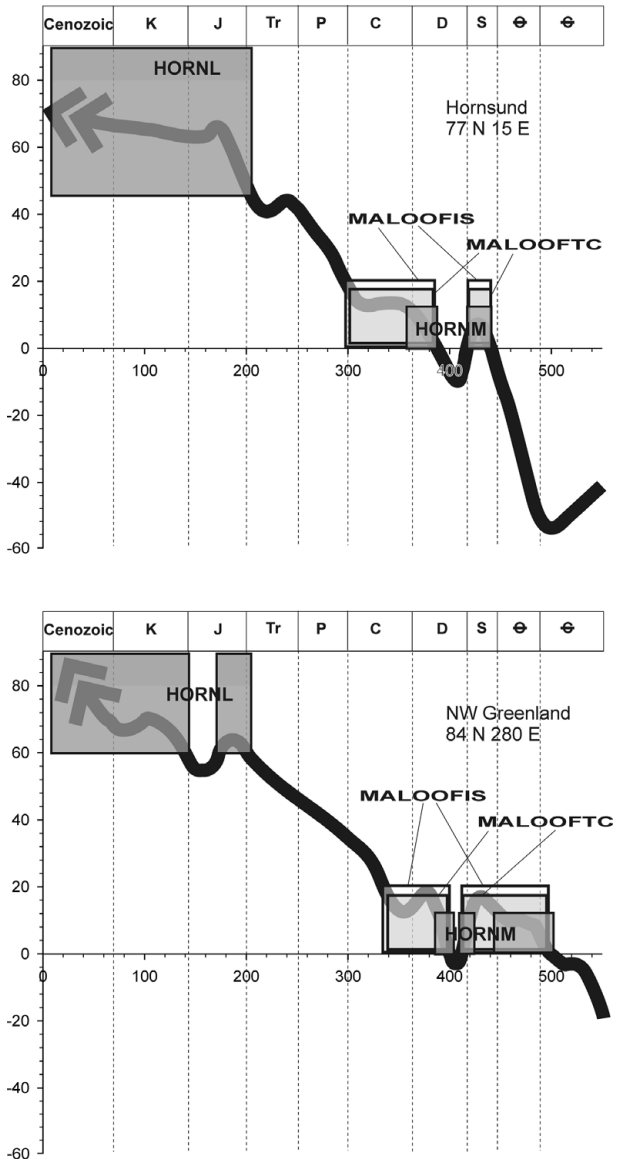

Figure 19. Palaeolatitudes of Central and Eastern terranes during magnetizations of palaeomagnetic directions from the Slaklidalen Fm (this study) and Grusdievbreen Fm (Maloof *et al*. 2006) with comparison to palaeolatitude curves of Hornsund and Northeastern Greenland. Palaeolatitude curves for Hornsund and Northeastern Greenland have been calculated, respectively, from Baltica and Laurentia APWPs, taken from GMAP 2002, 2003 palaeopole libraries. Palaeolatitudes of Central and Eastern terranes have been presented with confidence limits defined by D_p parameters; other abbreviations are as in Figure 16.

The present study has shown that at least two of the major terranes of Svalbard as defined by previous authors occupied similar geographical locations by Silurian time and the large-scale Late Devonian left lateral displacements previously proposed are not confirmed. To test the terrane models for other regions of Svalbard, which invoke large-scale left-lateral displacements on their bounding faults, it is evident that further palaeomagnetic studies, combined with better constrained isotopic ages of Caledonian tectonothermal events, are required from the various Svalbard terranes as well as their proposed counterparts in Greenland.

https://doi.org/10.1017/S0016756811000835 Published online by Cambridge University Press

Acknowledgements. This work was supported by the research project NO 3 P04D 037 25 of the Polish State Committee for Scientific Research. We are grateful to Dr Maciej Zalewski, Dr Piotr Głowacki and members of the XXII, XXV and XXVII expeditions to Polish Polar Station in Hornsund for the logistic support of palaeomagnetic field investigation during Arctic seasons 1999–2000, summer 2002 and summer 2004. We are also thankful to Dr Rafał Szaniawski and Dr Jacek Bednarek for field assistance during field investigations in Hornsund in seasons 2002 and 2004. We would like to express our thanks to Aleksandra Hołda-Michalska (Institute of Palaeobiology, Polish Academy of Sciences, Warszawa) for preparation of maps and figures. We would also like to thank the reviewers, Dr Michael S. Petronis, Dr Niels Abrahamsen and Dr Phil Leat for suggesting improvements to the original manuscript.

References

BARRÈRE, C., EBBING, J. & GERNIGON, L. 2009. Offshore prolongation of Caledonian structures and basement characterization in the western Barents Sea from geophysical modeling. *Tectonophysics* **470**, 71–88.

BIRKENMAJER, K. 1964. Devonian, Carboniferous and Permian formations of Hornsund, Vestspitsbergen. *Studia Polonica* **11**, 47–124.

BIRKENMAJER, K. 1975. Caledonides of Svalbard and plate tectonics. *Bulletin of the Geological Society of Denmark* **24**, 1–19.

BIRKENMAJER, K. & ORŁOWSKI, S. 1977. Olenellid fauna from the base of Lower Cambrian sequence in south Spitsbergen. *Norsk Polarinstitutt Årbok 1976*, 167–85.

BIRKENMAJER, K. 1978. Cambrian succession in south Spitsbergen. *Studia Geologica Polonica* **59**, 7–46.

BIRKENMAJER, K. 1990. *Geology of the Hornsund area, Spitsbergen. Explanations to the map 1:75000 scale*. Katowice: University of Silesia.

BREIVIK, A. J., MJELDE, R., GROGAN, P., SHIMAMURA, H., MURAI, Y., NISHIMURA, Y. & KUWANO, A. 2002. A possible Caledonide arm through the Barents Sea imaged by OBS data. *Tectonophysics* **355**, 67–97.

BREIVIK, A. J., MJELDE, R., GROGAN, P., SHIMAMURA, H., MURAI, Y. & NISHIMURA, Y. 2003. Crustal structure and transform margin development south of Svalbard based on ocean bottom seismometer data. *Tectonophysics* **369**, 37–70.

BREIVIK, A. J., MJELDE, R., GROGAN, P., SHIMAMURA, H., MURAI, Y. & NISHIMURA, Y. 2005. Caledonide development offshore–onshore Svalbard based on ocean bottom seismometer, conventional seismic, and potential field data. *Tectonophysics* **401**, 79–117.

BULLARD, E. C., EVERETT, J. E. & SMITH, A. G. 1965. The fit of the continents around the Atlantic. *Philosophical Transactions of the Royal Society of London, Ser. A*, **258**, 41–51.

BUTLER, R. F. 1992. *Paleomagnetism: Magnetic domains to geological terranes*. Boston: Blackwell Scientific Publications, 319 pp.

CLAESSON, K. C. 1979. Early Palaeozoic geomagnetism of Gotland. *Geologiska Foreningens I Stockholm Forhandlingar* **101**, 149–55.

COCKS, L. R. M. & TORSVIK, T. H. 2005. Baltica from late Precambrian to mid-Palaeozoic times: the gain and loss of a terrane's identity. *Earth Science Reviews* **72**, 39–66.

COX, A. & DOELL, R. R. 1960. Review of paleomagnetism. *Geological Society of America Bulletin* **71** (6), 645–768.

DEUTSCH, E. R. & PRASAD, J. N. 1987. Ordovician palaeomagnetic results from the St George and Table Head carbonates of western Newfoundland. *Canadian Journal of Earth Sciences* **24**, 1785–96.

DOUGLASS, D. N. 1988. Palaeomagnetics of Ringerike Old Red Sandstone and related rocks, southern Norway: implications for pre-Carboniferous separation of Baltica and British Terranes. *Tectonophysics* **148**, 11–27.

DUNLOP, D. J. & ÖZDEMIR, Ö. 1997. *Rock Magnetism Fundamentals and Frontiers*. New York, London and Cambridge: Cambridge University Press, 596 pp.

EIKEN, O. & AUSTEGARD, A. 1987. The Tertiary orogenic belt of Western Spitsbergen: seismic expressions of the offshore sedimentary basins. *Norges Geologisk Tidsskrift* **67**, 383–94.

ENKIN, R. J. 1994. *A Computer Program Package for Analysis and Presentation of Palaeomagnetic Data*. Sidney, BC: Pacific Geoscience Centre, Geological Survey of Canada.

ENKIN, R. J. & WATSON, G. S. 1996. Statistical analysis of palaeomagnetic inclination data. *Geological Journal International* **126**, 495–504.

FISHER, R. A. 1953. Dispersion on a sphere. *Proceedings of the Royal Society of London series A* **217**, 295–305.

GEE, D. G. & PAGE, L. 1994. Caledonian terrane assembly on Svalbard: new evidence from Ar/Ar dating in New Friesland. *American Journal of Science* **294**, 1166–86.

GEE, D. G. & TEBENKOV, A. M. 2004. Svalbard: a fragment of the Laurentian margin. In *The Neoproterozoic Timanide Orogen of Eastern Baltica* (eds D. G. Gee & V. Pease), pp. 191–206. Geological Society of London, Memoir 30.

GRAHAM, J. W. 1949. The stability and significance of magnetism in sedimentary rocks. *Journal of Geophysical Research* **54**, 131–67.

HALL, S. A. & EVANS, I. 1988. Palaeomagnetic study of the Ordovician Table Head Group, Port au Port Peninsula, Newfoundland. *Canadian Journal of Earth Sciences* **25**, 1407–19.

HALVORSEN, E. 1989. A palaeomagnetic pole position of Late Jurassic/Early Cretaceous dolerites from Hinlopenstretet, Svalbard, and its tectonic implications. *Earth and Planetary Letters* **94**, 398–408.

HAMBREY, M. J. 1982. Late Precambrian diamictites of northeastern Svalbard. *Geological Magazine* **119**, 527–51.

HARLAND, W. B. 1997. *The Geology of Svalbard*. Geological Society of London, Memoir 17, 521 pp.

HARLAND, W. B. & GAYER, R. A. 1972. The Arctic Caledonides and earlier oceans. *Geological Magazine* **109**, 289–314.

HARLAND, W. B. & WRIGHT, N. J. R. 1979. Alternative hypothesis for the pre-Carboniferous evolution of Svalbard. *Norsk Polarinstitutt Skrifter* **167**, 89–117.

HIRAJIMA, T., BANNO, S., HIROY, Y. & OHTA, Y. 1988. Phase petrology of eclogites and related rocks from Motalafjella high pressure metamorphic complex in Spitsbergen (Arctic Ocean) and its significance. *Lithos* **22**, 75–97.

HODYCH, J. P. 1989. Limestones of western Newfoundland that magnetized before Devonian folding but after Middle Ordovician lithification. *Geophysical Research Letters* **16**, 93–96.

HORSFIELD, W. T. 1972. Glaucophane schists of Caledonian age from Spitsbergen. *Geological Magazine* **109**, 29–36.

JELINEK, V. 1977. *The Statistical Theory of Measuring Anisotropy of Magnetic Susceptibility of Rocks and its Applications*. Brno: Geofizyka, 88 pp.

KĄDZIOŁKO-HOFMOKL, M. & KRUCZYK, J. 1976. Complete and partial self-reversal of natural remanent magnetization of basaltic rocks from Lower Silesia, Poland. *Pure and Applied Geophysics* **110**, 2031–40.

KIRSCHVINK, J. 1980. The least square line and plane and analysis of paleomagnetic data. *Geophysical Journal of the Royal Astronomical Society* **62**, 699–718.

LEWANDOWSKI, M. & ABRAHAMSEN, N. 2003. Paleomagnetic results from the Cambrian and Ordovician sediments of Bornholm (Denmark) and Southern Sweden and paleogeographical implications for Baltica. *Journal of Geophysical Research* **108** (B11), 2516, doi:10.1029/2002JB002281, 17 pp.

LEWANDOWSKI, M., WERNER, T. & NOWOŻYŃSKI, K. 1997. *PDA – a package of FORTRAN programs for palaeomagnetic data analysis, manuscript*. Warsaw: Institute of Geophysics, Polish Academy of Sciences.

LOWRIE, W. 1990. Identification of ferromagnetic minerals in a rock by coercivity and unblocking temperature properties. *Geophysical Research Letters* **17**, 159–62.

LYBERIS, N. & MANBY, G. 1999. Continental collision and lateral escape deformation in the lower and upper crust: an example from Caledonide Svalbard.*Tectonics* **18** (1), 40–63.

MANBY, G. M. 1978. Aspects of Caledonian metamorphism in central western Svalbard with particular reference to the glaucophane schists of Oscar II Land. *Polarforschung* **48**, 92–102.

MANBY, G. M. 1990. The petrology of the Harkerbreen Group, Ny Friesland, Svalbard: protoliths and tectonic significance. *Geological Magazine* **127**, 129–46.

MANBY, G. M. & LYBERIS, N. 1992. Tectonic evolution of the Devonian Basin of Northern Svalbard. *Norges Geologisk Tidsskrift* **72** no.1, 7–21.

MANBY, G. M., LYBERIS, N., CHOROWICZ, J. & THEIDIG, F. 1994. Post Caledonian tectonics along the Billefjorden Fault Zone, Svalbard and implications for the Arctic Region. *Geological Society of America Bulletin* **105**, 201–16.

MANECKI, M., HOLM, D. K., CZERNY, J. & LUX, D. 1998. Thermochronological evidence for Late Proterozoic (Vendian) cooling in southwest Wedel Jarlsberg Land, Spitsbergen. *Geological Magazine* **135**, 63–9.

MAZUR, S., CZERNY, J., MAJKA, J., MANECKI, M., HOLM, D., SMYRAK, A. & WYPYCH, A. 2009. A strike-slip terrane boundary in Wedel Jarlsberg Land, Svalbard, and its bearing on correlation of SW Spitsbergen with Pearya terrane and Timanide belt. *Journal of the Geological Society, London* **166**, 529–44.

MALOOF, A. C., HALVERSON, G. P., KIRSCHWINK, J. L., SCHRAG, D. P., WEISS, B. P. & HOFFMAN, P. F. 2006. Combined paleomagnetic, isotopic and stratigraphic evidence for true polar wander from the Neoproterozoic Akademikerbreen Group, Svalbard. *Geological Society of America Bulletin* **118**, 1099–124.

MCCABE, C., VAN DER VOO, R., WILKINSON, B. H. & DEVANEY, K. 1985. A Middle-Late Silurian palaeomagnetic pole from limestone reefs of the Wabash Formation (Indiana, USA). *Journal of Geophysical Research* **90**, 2959–65.

MCFADDEN, P. L. & MCELHINNY, M. W. 1990. Classification of the reversal test in palaeomagnetism. *Geophysical Journal International* **103**, 725–9.

MOSAR, J., TORSVIK, T. H. & the BAT team. 2002. Opening of the Norwegian and Greenland Seas: plate tectonics in Mid Norway since the Late Permian. In *BATLAS – Mid Norway Plate Reconstructions Atlas with Global and Atlantic Perspectives* (coord. E. A. Eide), pp. 48–59. Trondheim: Geological Survey of Norway.

OHTA, Y. 1979. Blueschists from Motalafjella, western Spitsbergen. *Norsk Polarinstitutt Skrifter* **167**, 171–217.

OHTA, Y. & DALLMANN, W. K. (eds) 1994. *Geological map of Svalbard, 1:100 000 sheet B12G, Torellbreen*. Norsk Polarinstitutt.

ROBERTS, D. 2003. The Scandinavian Caledonides: event chronology, palaeogeographic setting and likely modern analogues. *Tectonophysics* **365**, 283–99.

SKILBREI, J. R. 1992. Preliminary interpretation of aeromagnetic data from Spitsbergen, Svalbard Archipelago (76°–79° N): implications for structure of the basement. *Marine Geology* **106**, 53–68.

SRIVASTAVA, S. P. 1985. Evolution of the Eurasian Basin and its implications to the motion of Greenland along the Nares Strait. *Tectonophysics* **114**, 29–53.

SZLACHTA, K., MICHALSKI, K., BRZÓZKA, K., GÓRKA, B. & GAŁĄZKA-FRIEDMAN, J. 2008. Comparison of magnetic and Mössbauer results obtained for Palaeozoic rocks of Hornsund, Southern Spitsbergen, Arctic. Proceedings of the Polish Mössbauer Community Meeting 2008. *Acta Physica Polonica* **A 114** (6), 1675–82.

TARLING, D. H. & HROUDA, F. 1993. *The Magnetic Anisotropy of Rocks*. London: Chapman & Hall, 217 pp.

TAUXE, L. 1996. *Paleomagnetic Principles and Practice*. Dordrecht, Boston, London: Kluwer Academic Publishers, 299 pp.

TESSENSOHN, F., HENES-KUNST, F. & KRUMM, S. 2001. K/Ar dating attempts on rocks from the West Spitsbergen fold and thrust belt and the Central Basin. In *Intracontinental Fold Belts, CASE I: West Spitsbergen* (ed. F. Tessensohn), pp. 719–28. Hannover: Geologisches Jahrbuch Reihe B, Band B91, Polar Issue No. 7.

TORSVIK, T. H. 1984. Palaeomagnetism of the Foyers and Strontian granites, Scotland. *Physics of the Earth and Planetary Interior* **36**, 163–77.

TORSVIK, T. H. 1985. Palaeomagnetic results from the Peterhead granite, Scotland: implication for regional late Caledonian magnetic overprinting. *Physics of the Earth and Planetary Interior* **39**, 108–16.

TORSVIK, T. H. & COCKS, L. R. M. 2005. Norway in space and time: a centennial cavalcade. *Norwegian Journal of Geology* **85**, 73–86.

TORSVIK, T. H. & REHNSTRÖM, E. F. 2001. Cambrian paleomagnetic data from Baltica: implications for true polar wander and Cambrian palaeogeography. *Journal of the Geological Society, London* **158**, 321–9.

TORSVIK, T. H., SMETHURST, M. A., MEERT, J. G., VAN DER VOO, R., MCKERROW, W. S., BRASIER, M. D., STURT, B. A. & WALDERHAUG, H. J. 1996. Continental break-up and collision in the Neoproterozoic and Palaeozoic – a tale of Baltica and Laurentia. *Earth Science Reviews* **40**, 229–58.

TRENCH, A. & TORSVIK, T. H. 1991. The Lower Palaeozoic apparent polar wander path for Baltica: palaeomagnetic data from Silurian limestones of Gotland, Sweden. *Geophysical Journal International* **107**, 373–9.

TURNELL, H. B. 1985. Palaeomagnetism and Rb-Sr ages of the Ratagan and Comrie intrusions. *Geophysical Journal of the Royal Astronomical Society* **83**, 363–78.

VAN DER VOO, R. 1993. *Paleomagnetism of the Atlantic, Tethys and Iapetus Oceans*. Cambridge: Cambridge University Press, 424 pp.

VINCENZ, S. A., COSSACK, D., DUDA, S. J., BIRKENMAJER, K., JELEŃSKA, M., KĄDZIOŁKO-HOFMOKL, M. & KRUCZYK, J. 1981. Palaeomagnetism of some late Mesozoic dolerite dikes of South Spitsbergen. *Geophysical Journal of the Royal Astronomical Society* **67**, 599–614.

VINCENZ, S. A., JELEŃSKA, M., AIINEHSAZIAN, K. & BIRKEMAJER, K. 1984. Palaeomagnetism of some late Mesozoic dolerite sills of East Central Spitsbergen, Svalbard Archipelago. *Geophysical Journal of the Royal Astronomical Society* **78**, 751–73.

https://doi.org/10.1017/S0016756811000835 Published online by Cambridge University Press